Article

Neuron

Increased Cocaine Motivation Is Associated with Degraded Spatial and Temporal Representations in IL-NAc Neurons

Graphical Abstract

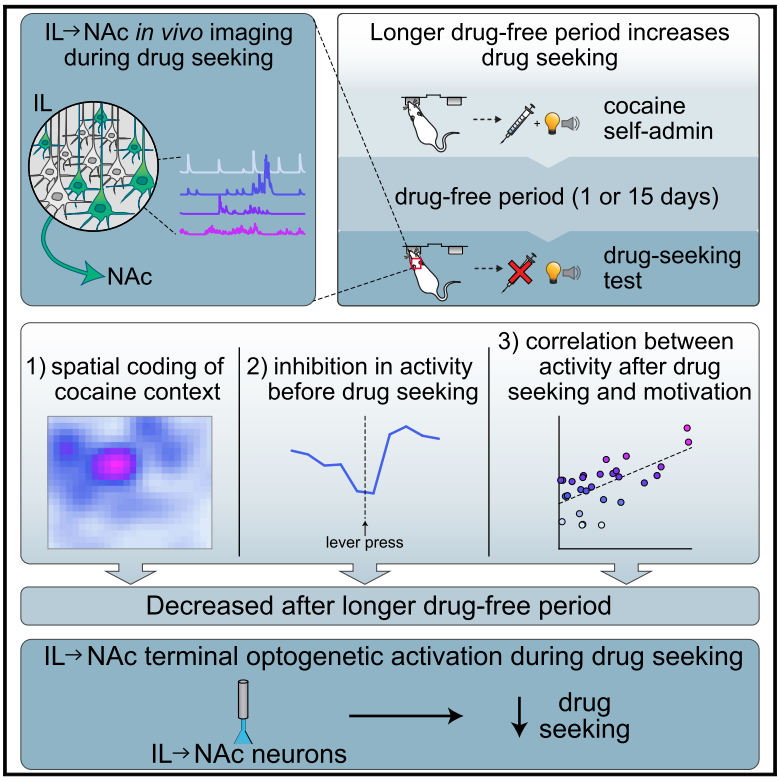

Highlights

- Cellular resolution imaging of IL-NAc projection neurons in rats
- IL-NAc neurons display spatial and temporal selectivity during drug seeking
- After a drug-free period, drug motivation is high and neural coding is degraded
- Activation of IL-NAc neurons reduces drug seeking

Authors

Courtney M. Cameron, Malavika Murugan, Jung Yoon Choi, Esteban A. Engel, Ilana B. Witten

Correspondence

iwitten@princeton.edu

In Brief

Cameron et al. report that spatial and temporal representations in IL-NAc neurons during drug seeking are degraded after a drug-free period. The disengagement of this "anti-relapse" projection may contribute to heightened drug seeking that results from a drug-free period.

Cameron et al., 2019, Neuron *103*, 1–12
July 3, 2019
https://doi.org/10.1016/j.neuron.2019.04.015

CellPress

Please cite this article in press as: Cameron et al., Increased Cocaine Motivation Is Associated with Degraded Spatial and Temporal Representations in IL-NAc Neurons, Neuron (2019), https://doi.org/10.1016/j.neuron.2019.04.015

Neuron
Article

Increased Cocaine Motivation Is Associated with Degraded Spatial and Temporal Representations in IL-NAc Neurons

Courtney M. Cameron,[1] Malavika Murugan,[1] Jung Yoon Choi,[1,2] Esteban A. Engel,[1] and Ilana B. Witten[1,2,3,*]
[1]Princeton Neuroscience Institute, Princeton University, Princeton, NJ 08544, USA
[2]Department of Psychology, Princeton University, Princeton, NJ 08544, USA
[3]Lead Contact
*Correspondence: iwitten@princeton.edu
https://doi.org/10.1016/j.neuron.2019.04.015

SUMMARY

Craving for cocaine progressively increases in cocaine users during drug-free periods, contributing to relapse. The projection from the infralimbic cortex to the nucleus accumbens shell (IL-NAc) is thought to inhibit cocaine seeking. However, it is not known whether and how IL-NAc neurons contribute to the increased motivation associated with a drug-free period. We first performed cellular resolution imaging of IL-NAc neurons in rats during a drug-seeking test. This revealed neurons with spatial selectivity within the cocaine-associated context, a decrease in activity around the time of cocaine seeking, and an inverse relationship between cocaine-seeking activity and subsequent cocaine motivation. All these properties were reduced by a drug-free period. Next, we transiently activated this projection, which resulted in reduced drug seeking, regardless of the drug-free period. Taken together, this suggests that altered IL-NAc activity after a drug-free period may enhance cocaine motivation without fundamentally altering the projection's ability to inhibit drug seeking.

INTRODUCTION

Cocaine addiction is characterized by a continuous cycle of excessive drug use, intermittent drug-free periods, and relapse (Gawin, 1991). High rates of relapse may be caused, in part, by a progressive increase in cocaine craving during drug-free periods ("incubation of cocaine craving") (Conrad et al., 2008; Grimm et al., 2001; Tran-Nguyen et al., 1998; Wang et al., 2018). Thus, an understanding of the mechanisms through which a drug-free period contributes to heightened cocaine motivation could prove valuable in recognizing and preventing vulnerability to relapse.

The medial prefrontal cortex and the nucleus accumbens (NAc) are thought to be critical in controlling drug seeking (Calu et al., 2007; Cameron and Carelli, 2012; Chang et al., 2000; Chen et al., 2013; De Biasi and Dani, 2011; Hwa et al., 2017; Janak et al., 1999; Kalivas and Volkow, 2011; Koya et al., 2012; Lee et al., 2016; Ma et al., 2018; McGlinchey et al., 2016; Phillips et al., 2003; Robbins et al., 2010; Robledo and Koob, 1993; Saunders et al., 2013; Walker et al., 2018). Of particular interest, activity in the descending projection from the infralimbic cortex to the NAc (IL-NAc) is thought to inhibit drug seeking, suggesting a potential "anti-relapse" function of this projection (Augur et al., 2016; Gutman et al., 2017; Ma et al., 2014; Pascoli et al., 2014; Peters et al., 2008; Sun et al., 2014).

This ability of IL-NAc neurons to inhibit drug seeking raises the important question of what information these neurons encode and whether these neurons contribute to the increase in cocaine motivation that is associated with a drug-free period. No prior study has selectively recorded from this projection-defined population during drug seeking, and thus it is unknown whether and how these neurons represent drug-seeking behavior.

One possibility is that a drug-free period increases cocaine motivation in part by altering or reducing the representation of cocaine-related information in IL-NAc neurons. Testing this would involve selectively recording from these neurons during drug seeking and determining whether and how this activity was altered by a drug-free period. Another possibility is that the increase in cocaine motivation caused by a drug-free period is due in part to a decrease in the *ability* of IL-NAc neurons to suppress drug-seeking behavior. This could be mediated by plasticity either in IL-NAc synaptic terminals or in downstream circuits (Ma et al., 2014; Pascoli et al., 2014). Testing this would involve determining whether the effect of manipulating activity in this projection on drug seeking is reduced by a drug-free period. No prior study has examined whether the behavioral consequences of activity in IL-NAc neurons is altered by a drug-free period.

Thus, we sought to clarify what IL-NAc neurons represent during cocaine seeking, and whether and how this may be altered by a drug-free period. We recorded and manipulated IL-NAc activity in rats that had been trained to self-administer cocaine. This revealed neurons with spatial selectivity within the cocaine-associated context, an overall decrease in activity around the time of cocaine seeking, and an inverse relationship between cocaine-seeking-related activity and subsequent cocaine motivation. Interestingly,

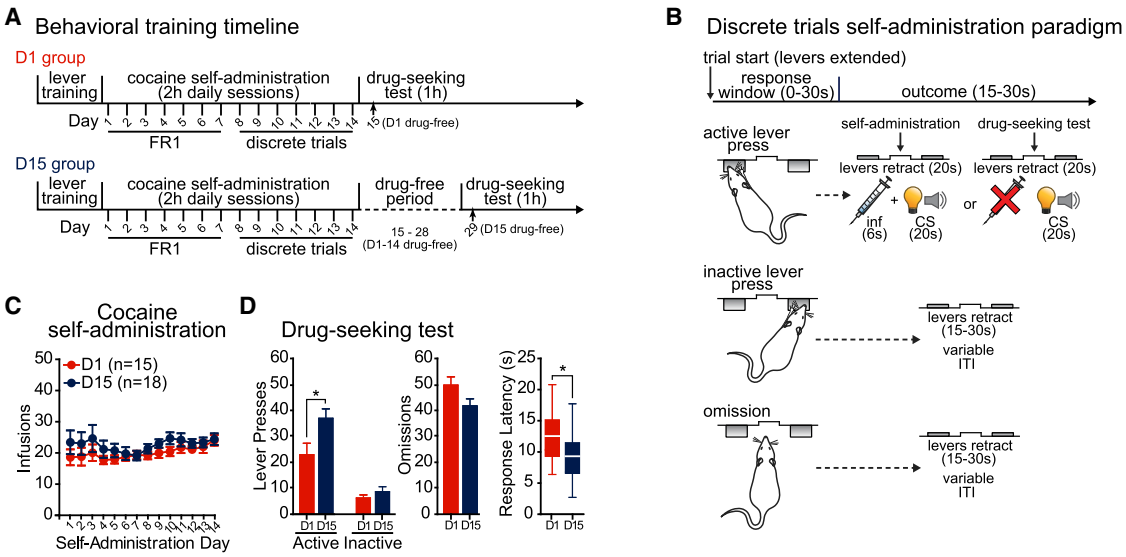

Figure 1. A Longer Drug-free Period Results in Greater Drug Seeking following Cocaine Self-Administration

(A) Schematic of behavioral training timeline.

(B) After 7 days of traditional FR1 cocaine self-administration, rats were trained for 7 additional days on a modified FR1 paradigm that introduced discrete trials. The start of each trial was signaled by extension of the levers into the chamber, and rats could make 1 of 3 responses: active lever press, inactive lever press, or omission. Active lever presses resulted in cocaine infusion, CS presentation, and lever retraction. Inactive lever presses resulted in lever retraction and a variable inter-trial-interval (ITI). Omissions occurred if a rat made no response for 30 s and resulted in lever retraction and a variable ITI. The drug-seeking test was performed using the same discrete trials paradigm, but no cocaine (only CS) was delivered in response to an active lever press.

(C) Over 14 days of cocaine self-administration, rats in both groups (D1: n = 15; D15: n = 18) self-administered a similar number of cocaine infusions (mean ± SEM; main effect of D1/D15 group: $F_{(1,403)} = 1.89$, $p = 0.18$).

(D) Incubation of cocaine craving. Rats that experienced a 15-day drug-free period (D15) made more active lever presses (mean ± SEM) and had faster response latencies during the drug-seeking test (median, box represents 25th and 75th percentiles, bars represent minimum and maximum values). *$p < 0.05$, two-tailed t test.

See also Figure S1.

all of these properties were reduced by a longer drug-free period (15 days versus 1 day). On the other hand, transient activation of these neurons resulted in reduced drug seeking that was unaffected by the length of the drug-free period. Together, this suggests that a degraded representation of cocaine-related information in IL-NAc neurons may contribute to increased cocaine motivation in animals that have undergone a longer drug-free period.

RESULTS

A Drug-free Period Enhances Drug Seeking following Cocaine Self-Administration

We trained rats to press a lever ("active lever") to receive an intravenous infusion of cocaine (0.33 mg/0.2 mL/infusion [inf], ~1 mg/kg) paired with a tone-houselight conditioned stimulus ("CS") and lever retraction (Figures 1A and 1C). A second lever was available but had no programmed consequence ("inactive lever"; Figure S1A).

Training consisted of daily 2-h sessions for 14 consecutive days. The first 7 days of training were performed under a fixed ratio 1 (FR1) schedule of reinforcement. On days 8–14, rats were trained on a modified FR1 schedule that introduced discrete trials (Figure 1B). This novel trial-based self-administration paradigm allowed us to examine several drug-seeking behaviors—in particular, response latency and response omission—which are not accessible in traditional self-administration paradigms that use a continuous reinforcement schedule.

After a 1-day (D1 group) or 15-day (D15 group) drug-free period, we assessed rats' cocaine motivation during a single cue-induced drug-seeking test. In this test, pressing the active lever (a measure of drug seeking) resulted in presentation of the CS previously paired with drug infusion, but no cocaine was delivered. As expected, drug seeking was higher after the longer drug-free period. Rats in the D15 group made significantly more active lever presses and had faster response latencies compared to rats in the D1 group, consistent with an increased motivation to seek cocaine (number of active presses: D1: 22.93 ± 4.42, D15: 36.94 ± 3.70, two-tailed t test: $t_{(31)} = 2.45$, $p = 0.020$; response latency: D1: 12.87 ± 1.02 s, D15: 9.33 ± 0.85 s, two-tailed t test: $t_{(31)} = 2.70$, $p = 0.011$; Figure 1D).

Cellular Resolution Imaging of IL-NAc Neurons during Drug Seeking

To evaluate how neural correlates in IL-NAc neurons may be affected by the drug-free period, we expressed the calcium indicator GCaMP6f selectively in NAc-projecting IL neurons in rats to image these neurons (similar approaches employed recently in

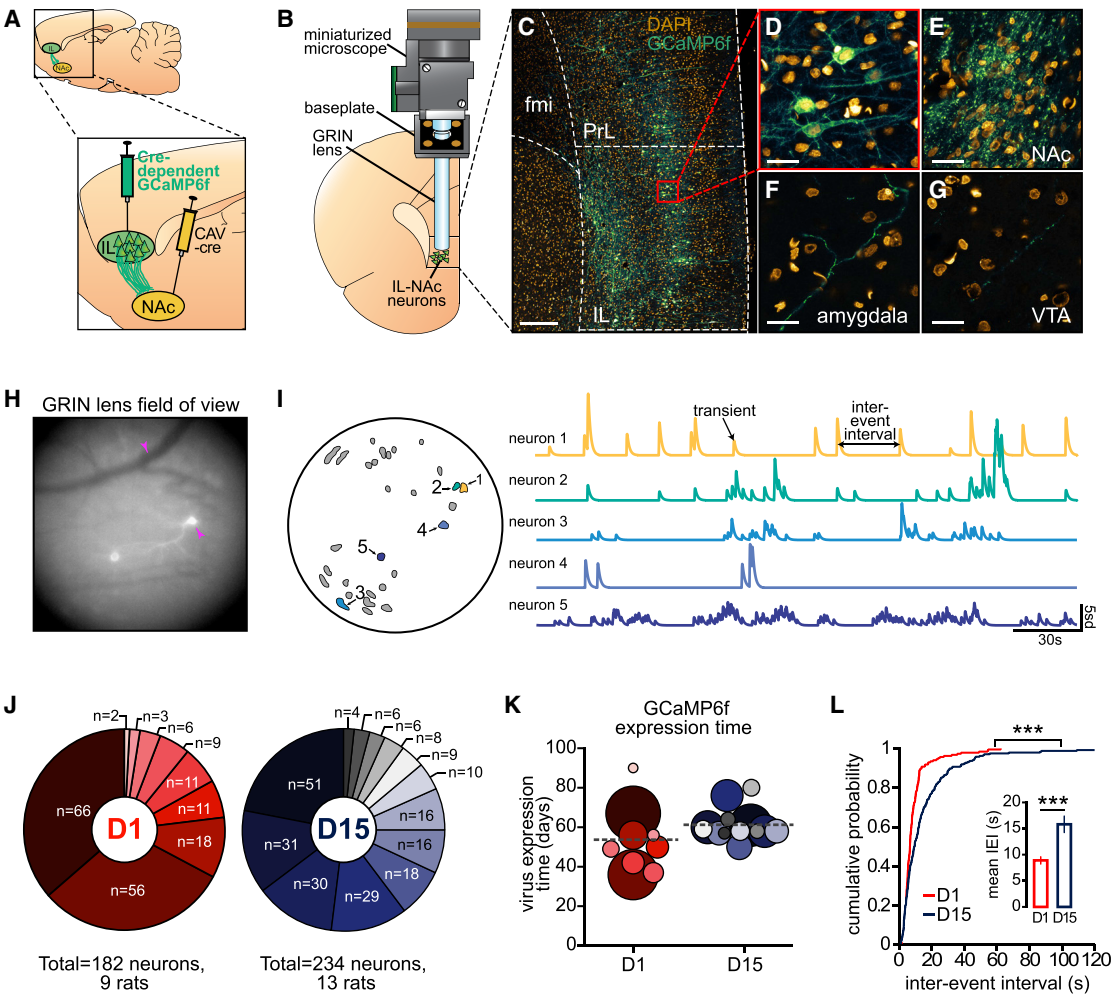

Figure 2. Cellular Resolution Calcium Imaging of NAc-Projecting IL Neurons

(A) Targeting of GCaMP6f to IL-NAc neurons. Retrograde CAV2-Cre virus was injected in the NAc and Cre-dependent AAV5-GCaMP6f in the IL.

(B) Imaging setup including GRIN lens placement in IL.

(C) GCaMP6f expression in IL-NAc neurons (green) and DAPI staining of cell nuclei (gold). PrL, prelimbic cortex; IL, infralimbic cortex; fmi, forceps minor of the corpus callosum. Scale bar, 250 μm.

(D) Confocal image of IL-NAc neurons showing nuclear exclusion of GCaMP6f. Scale bar, 25 μm.

(E) Dense GCaMP6f terminal expression in the NAc shell. Scale bar, 25 μm.

(F and G) Sparse terminal expression in (F) amygdala and (G) VTA. Scale bars, 25 μm.

(H) Grayscale projection from recording through a GRIN lens in a representative rat. Magenta arrows denote blood vessel (black) and active neuron (white).

(I) Left: field of view from this recording with identified neurons shown in gray. Right: fluorescence traces of example neurons (color coded on left).

(J) Pie charts showing number of neurons recorded per rat (D1: n = 182 neurons, 9 rats; D15: n = 234 neurons, 13 rats).

(K) GCaMP6f expression time during each imaging experiment. The sizes of circles are proportional to the number of neurons recorded in each animal.

(L) Cumulative density function and bar graph (mean ± SEM; inset) of the mean inter-event interval (IEI) for all recorded neurons (D1: n = 182; D15: n = 234). The mean IEI of neurons was increased after a drug-free period.

***$p < 0.001$, two-tailed t test for D1 compared to D15; ***$p < 0.000001$, two-sample Kolmogorov-Smirnov (K-S) test for D1 versus D15.

See also Figure S1.

mice in other neural populations: (Barbera et al., 2016; Murugan et al., 2017; Otis et al., 2017; Pinto and Dan, 2015; Siciliano and Tye, 2019; Xia et al., 2017; Ziv et al., 2013)). We injected a retrogradely traveling CAV2 virus expressing Cre recombinase into the NAc, and a Cre-dependent AAV2/5 viral construct expressing GCaMP6f into the IL (Figure 2A). Cell bodies in the IL expressed GCaMP6f (Figures 2C and 2D), and dense terminal expression was observed in the NAc (Figure 2E), indicating that IL-NAc neurons were labeled. In addition, very sparse terminal expression was visible in the amygdala (Figure 2F) and ventral tegmental area (VTA) (Figure 2G), suggesting that IL-NAc neurons sent relatively sparse collaterals to these other downstream targets, consistent with recent findings (Bloodgood et al., 2018).

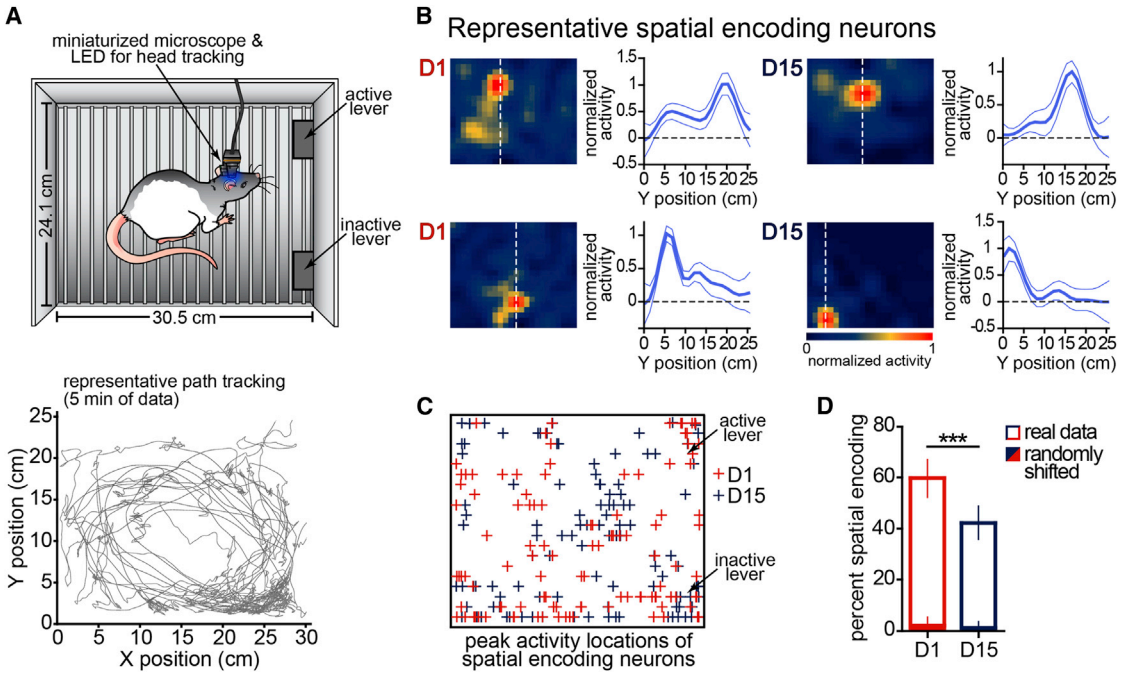

Figure 3. A Drug-free Period Reduces Spatial Coding of the Cocaine Context in IL-NAc Neurons

(A) Top: schematic showing dimensions of operant chamber. A blue LED was used for head-tracking. Bottom: example path of a single rat (5 min of data).
(B) Example spatial fields of significant neurons ($p < 0.01$; normalized to peak activity). Line plots represent vertical slice through peak with error bars (±2 SD).
(C) Peak activity locations of spatial neurons (D1: n = 109; D15: n = 99). The place fields of these neurons were located throughout the operant chamber.
(D) The fraction of neurons with significant spatial coding decreased after a drug-free period (D1: n = 109/182, 59.89%; D15: 99/234, 42.31%). When calcium data were randomly shifted relative to spatial position data, very few neurons showed significant spatial encoding (D1: n = 4/182, 2.2%; D15: n = 3/234, 1.3%). Error bars represent 95% confidence interval for binomial distribution. ***$p < 0.001$, Fisher's exact test.
See also Figure S2.

A week after virus injection, a gradient refractive index (GRIN) lens (or GRIN lens with prism attached) was implanted above the IL (Figure 2B). Following self-administration training, the lens was coupled to a head-mounted miniaturized microscope to record single-cell activity of GCaMP-expressing IL-NAc neurons as rats performed the drug-seeking test (D1 group: n = 182 neurons, 9 rats; D15 group: n = 234 neurons, 13 rats; Figures 2H–2K; Figures S1F and S1G; example videos in Videos S1 and S2).

We found that the length of the drug-free period altered the pattern of calcium events in IL-NAc neurons. Specifically, the average inter-event interval (time between transients; calculated across the entire recording session) was increased in the D15 compared to D1 group (15.80 ± 1.55 s versus 8.90 ± 0.67 s; two-tailed t test: $t_{(414)} = 3.73$, $p = 0.00021$; a mixed-effect linear regression with D1/D15 group as fixed effect and rat identity as a random effect found a similar trend: $F_{(1,414)} = 3.37$, $p = 0.067$, see details in STAR Methods; Figure 2I). However, the overall frequency of events was not significantly different between the D1 and D15 groups (10.53 ± 0.51 versus 9.51 ± 0.63 transients/min; two-tailed t test: $t_{(414)} = 1.22$, $p = 0.22$). This is likely because neurons in the D15 group tended to have periods with high event frequency and also periods with low event frequency, in contrast to neurons in the D1 group, which had less variability in event frequency. Consistent with this, the SD of inter-event interval was higher for the D15 compared to D1 neurons (36.75 ± 3.60 s versus 19.57 ± 1.66 s; two-tailed t test: $t_{(414)} = 3.96$, $p < 0.0001$).

A Drug-free Period Results in Fewer IL-NAc Neurons with Spatial Selectivity

We first examined whether IL-NAc neurons had spatial selectivity within the cocaine-associated environment, inspired by previous findings of spatial fields in rodent medial prefrontal cortex (mPFC) (Murugan et al., 2017; Spellman et al., 2015; Wang et al., 2015; schematic of chamber and example position tracking, Figure 3A). We found that a large fraction of IL-NAc neurons had spatially selective responses during the drug-seeking test (example neurons, Figure 3B). The spatial fields of these neurons were distributed throughout the chamber in both the D1 and D15 groups (Figure 3C). Interestingly, the proportion of neurons with significant spatial selectivity was substantially reduced by the longer drug-free period (D1: 59.9%, n = 109/182, D15: 42.3%, n = 99/234; Fisher's exact test: p = 0.0005, Figure 3D; see Methods for definition of significant spatial selectivity), suggesting a general deficit in encoding of the cocaine context following a drug-free period.

Before the Drug-Seeking Action, There Is a Net Decrease in IL-NAc Activity, although This Is Less Pronounced after a Longer Drug-free Period

We next examined neural activity related to our primary measure of drug seeking: active lever presses. We classified a

neuron as significantly time locked to the active lever press if the minimum or maximum of its activity within ±5 s of the active lever press differed from the null distribution obtained from randomly shifting neural activity relative to the times of lever presses (see STAR Methods; example time-locked neurons in Figure 4A).

Interestingly, a larger proportion of significantly time-locked neurons were inhibited (INH; 60.38%, n = 64/106) rather than excited (EXT; 39.62%, n = 42/106) around the time of the lever press (two-tailed exact binomial: p = 0.041; Figure 4B). This inhibition around the time of the active lever press was evident not only when considering the fraction of significantly time-locked neurons (Figure 4B), but also when considering the average (*Z* scored) activity across all recorded neurons (Figure 4C).

The fact that the average IL-NAc activity decreases at the time of the active lever press implies that a decrease in activity in this projection may be permissive for drug seeking. In other words, it provides correlative evidence for the idea that activity in IL-NAc is associated with reduced drug seeking. Further supporting the idea that activity in IL-NAc neurons is inversely related to drug seeking, we found that activity at the start of trials in which rats omitted to press a lever (omission trials) was higher on average than activity at the start of trials on which animals made an active lever press (paired two-tailed t test: $t_{(415)} = 3.33$, p = 0.00095; Figure S4D).

Is this decrease in activity around the active lever press affected by the length of the drug-free period? Although a similar fraction of neurons displayed significantly time-locked activity related to the active lever press in both the D1 and D15 groups (D1: 21.43%, n = 39/182; D15: 29.49%, n = 69/234; Fisher's exact test: p = 0.07; Figure 4D), the distribution of excited versus inhibited neurons was altered by the length of the drug-free period (chi-square: $X^2_{(4)} = 12.47$ [n = 414], p = 0.014; Figure 4D). Specifically, we observed that fewer neurons were excited before an active press in the D1 compared to D15 group (D1: 0.56% EXT before, n = 1/180; D15: 5.13% EXT before, n = 12/234; Fisher's exact test: p = 0.043; Figures 4E and 4F, right). Similarly, we observed that the extent of inhibition before the active lever press was on average greater in the D1 than the D15 group (2-factor mixed ANOVA with group and time as factors: group × time interaction: $F_{(9,576)} = 2.41$, p = 0.011; D1 versus D15 simple main effect, p = 0.019, 0.030; Figures 4F and 4G, left).

These differences suggest that although inhibition was present around the time of the lever press in both the D1 and D15 groups, it may be more pronounced in D1 animals. Further supporting this claim, when considering all neurons that were significantly modulated by the active lever press, the extent of inhibition was greater for D1 compared to D15 (2-factor mixed ANOVA with group and time as factors: group × time interaction: $F_{(9,954)} = 3.62$, p = 0.00019; D1 versus D15 simple main effect, p = 0.0029, 0.031; Figure 4H). Similarly, we observed more inhibition before the lever press for D1 than D15 neurons when we considered the entire population of recorded neurons, rather than only those with significant active lever press responses (2-factor mixed ANOVA with group and time as factors: group × time interaction: $F_{(9,3726)} = 4.26$, p < 0.0001; D1 versus D15 simple main effect, p = 0.036; a mixed-effect linear regression with D1/D15 group as fixed effect and rat identity as a random effect: D1 versus D15: $F_{(1,414)} = 7.61$, p = 0.0061, see details in STAR Methods; Figure 4I).

Similar to the net decrease in activity associated with the active lever press (Figures 4B and 4C), we also observed a decrease in activity around inactive lever presses (compared to a null distribution generated by randomly shifting the calcium traces relative to the lever press times: p < 0.05; Figure S3D, right). However, in individual neurons, statistically significant modulation with respect to the inactive lever was observed less frequently (Figure S3B).

Immediately after Drug Seeking, IL-NAc Activity Is Inversely Related to Subsequent Motivation to Seek Drug, although This Is Reduced by a Drug-free Period

Although the pattern of activity before an active lever press was altered by a drug-free period (Figure 4), most neurons with significant time-locked responses had minima (for INH neurons) or maxima (for EXT neurons) that occurred *after* the lever press (not before; Figure 5A). The period immediately after a lever press may be important for providing feedback about the outcome (or identity) of the previous action. Therefore, we asked whether activity after the lever press was predictive of subsequent drug-seeking behavior. Indeed, we found that across the population of recorded neurons, the peak activity after an active lever press was positively correlated with the latency to make a press on the subsequent trial in the D1 group; however, this relationship was not present in the D15 group (D1 median correlation coefficient different from zero: Wilcoxon signed-rank test: z = 4.45, p < 0.00001; D15 median not different from zero: Wilcoxon signed-rank test: z = −0.40, p = 0.69; two-sample Kolmogorov-Smirnov [K-S] test D1 versus D15: k = 0.20, p = 0.00091; a mixed-effect linear regression with D1/D15 group as fixed effect and rat identity as a random effect: D1 versus D15: $F_{(1,380)} = 11.97$, p = 0.00060, see details in STAR Methods; Figures 5B and 5C).

Given that longer response latencies are indicative of lower drug-seeking motivation, these data provide additional support for the idea that higher IL-NAc activity suppresses subsequent drug-seeking behavior (e.g., inhibition in activity before an active lever press Figures 4C and 4E–4I; higher activity on omission compared to press trials, Figures S4A–S4F).

To control for the possibility that the observed correlation between neural activity and subsequent lever press latency can be better explained by time-dependent changes in behavior and/or in neural activity, we also correlated neural activity with time in the session (instead of lever press latency). However, activity after the lever press did not correlate with time in the session in the D1 group, nor was the correlation significantly different between groups (Figures S4G and S4H).

In summary, our imaging experiments revealed that a drug-free period altered IL-NAc encoding of drug-seeking behavior in multiple ways, including: (1) a reduction in spatial selectivity (Figure 3), (2) a reduction in inhibition preceding an active lever press (Figure 4), and (3) a disruption in the relationship between cocaine-seeking-related activity and cocaine motivation on the subsequent trial (Figure 5).

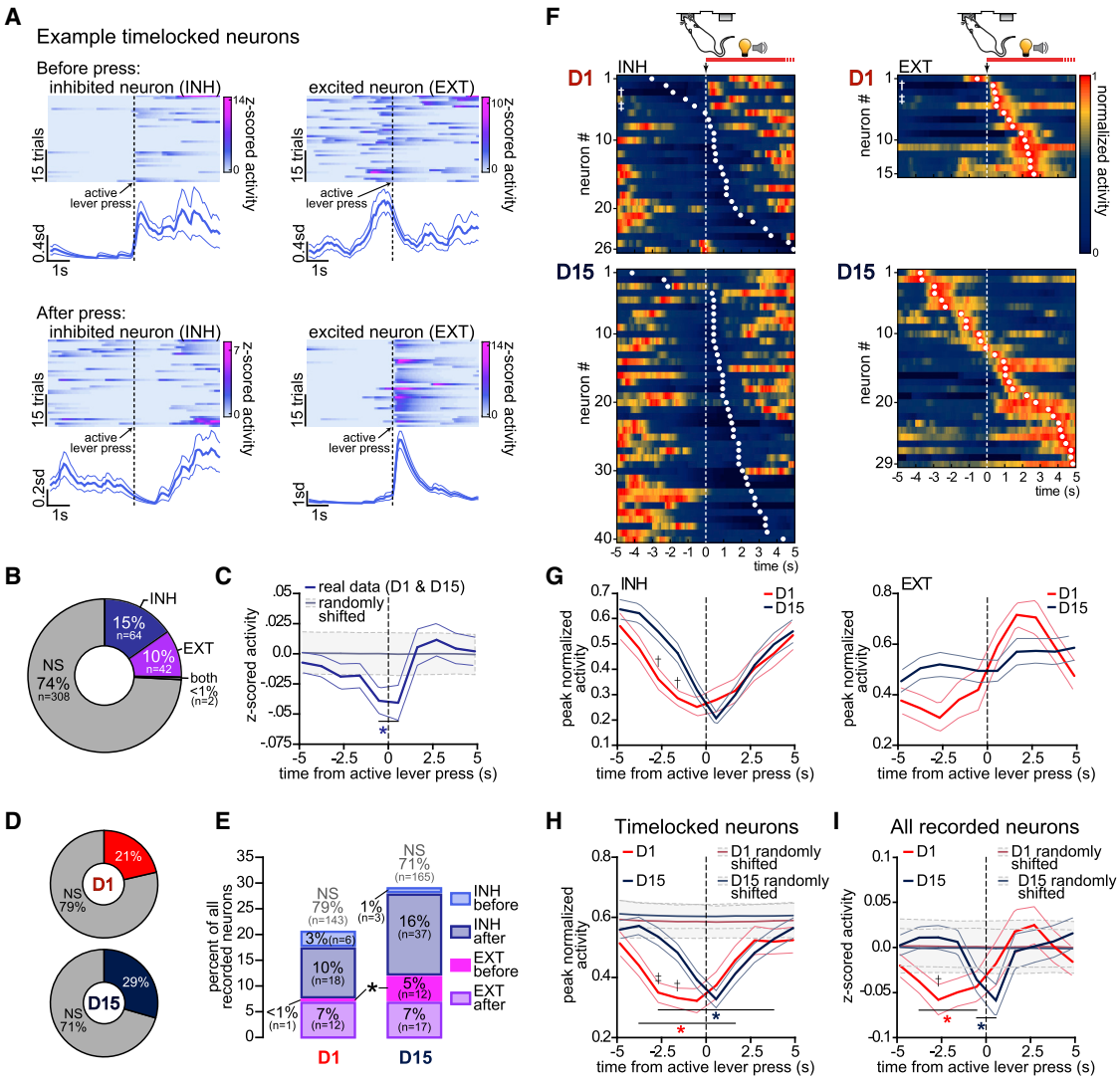

Figure 4. Before the Drug-Seeking Behavior (Active Lever Press), There Is a Net Decrease in IL-NAc Activity, Although This Is Lessened by a Drug-free Period

(A) Example neurons with significant time-locked responses. Heatmaps represent *Z*-scored activity on active lever press trials (10 s window; dotted line at time of press). Traces below show mean ± SEM activity for all active lever press trials. Neurons were divided into 4 response types: inhibited before a press, excited before a press, inhibited after a press, or excited after a press.

(B) Across both the D1 and D15 groups, 15.38% (n = 64/416) of neurons were inhibited (INH), 10.10% (n = 42/416) were excited (EXT), and 0.48% (n = 2/416) exhibited both an INH and EXT response. 74.04% (n = 308/416) of neurons had no significant time-locked response relative to active lever press.

(C) Mean ± SEM *Z*-scored activity of all recorded neurons (n = 416) as well as randomly shifted data (mean ± 2 SD; 1,000 shifted iterations). There was a decrease in activity around the time of active lever press. *p < 0.05, real data compared to shifted.

(D) In the D1 group, 21.43% (n = 39/182) of neurons were significantly time locked to active lever press. In the D15 group, 29.49% (n = 69/234) were significantly time locked.

(E) After a drug-free period, more neurons were excited before the active lever press. *p < 0.05, Fisher's exact test for D1 versus D15 EXT before. D1: 3.33% INH before, n = 6/180; 10% INH after, n = 18/180; 0.56% EXT before, n = 1/180; 6.67% EXT after, n = 12/180; 79.44% not significant, n = 143/180; D15: 1.28% INH before, n = 3/234; 15.81% INH after, n = 37/234; 5.13% EXT before, n = 12/234; 7.26% EXT after, n = 17/234; 70.51% not significant, n = 165/234. 2 neurons in the D1 group exhibited both an EXT and INH response and were not included in this analysis.

(F) Activity traces (normalized to peak) of all significant time-locked neurons (INH on left, D1: n = 26, D15, n = 40; EXT on right, D1: n = 15, D15: n = 29). Dotted line indicates time of active lever press and white dots indicate time of minima or maxima. The 2 neurons with both EXT and INH responses are plotted in both groups (traces indicated with † and ‡).

(G) Mean ± SEM activity (peak normalized) of all significant INH (left) and EXT (right) time-locked neurons. Left: inhibition before active lever press was reduced in the D15 compared to D1 group. †p < 0.05, simple main effect D1 versus D15. Right: group × time interaction: $F_{(9,378)} = 4.402$, p < 0.0001; D1 versus D15 simple main effect not significant at any time point.

(legend continued on next page)

IL-NAc Activity Reduces Drug Seeking, Regardless of the Length of the Drug-free Period

Next, to directly assess the effect of IL-NAc activity on drug-seeking behavior and determine whether this effect was altered by a drug-free period, we used optogenetics to activate these neurons. An adeno-associated virus (AAV2/5) expressing ChR2-yellow fluorescent protein (YFP) or YFP-only (control rats) was injected into the IL (Figure 6A), and optical fibers were implanted above the NAc shell (Figure 6B). Similar to the imaging experiment (Figures 1, 2, 3, 4, 5), rats were trained to self-administer cocaine and then experienced either a 1- (D1 group) or 15-day (D15 group) drug-free period before a 2-h drug-seeking test (Figures 6C and 6D). During the drug-seeking test, optical stimulation (~10 mW, 20 Hz, 5-ms pulses) was applied during 50% of trials (randomly selected), allowing us to probe the effects of activation of this projection in a within-subject manner.

Given that activation of the IL-NAc projection is itself rewarding (i.e., supports intracranial self-stimulation, ICSS; Figure S6A), we employed a stimulation paradigm that was not contingent on the rats' lever press behavior to avoid any possible confound of a self-stimulation effect. Specifically, stimulation began at trial start (lever presentation) and lasted for the duration of the trial, ending at the next trial start.

Based on previous manipulations of this circuit (Augur et al., 2016; Gutman et al., 2017; Ma et al., 2014; Pascoli et al., 2014; Peters et al., 2008), as well as our finding of an overall decrease in activity in IL-NAc neurons before drug seeking, we predicted that activation of IL-NAc neurons would decrease drug seeking. Indeed, we found that active lever pressing was decreased on stimulation (stim) versus no stimulation (no stim) trials (2-factor mixed ANOVA with D1/D15 and stim-no stim as factors: main effect of stimulation: $F_{(1,34)} = 19.06$, $p = 0.0001$; Figure 6E, top). Stimulation did not significantly alter omission rate ($F_{(1,34)} = 1.40$, $p = 0.24$); however, it did increase inactive lever pressing (main effect of stimulation: $F_{(1,34)} = 8.45$, $p = 0.0064$; Figure 6E, top).

This decrease in drug seeking as a result of activating IL-NAc neurons was comparable in both the D1 and D15 groups. Although the D15 group showed the expected increase in drug seeking (more active lever presses: main effect of D1 versus D15: $F_{(1,34)} = 5.71$, $p = 0.023$; fewer omissions: $F_{(1,34)} = 5.02$, $p = 0.032$), there was no significant interaction between group (D1/D15) and stimulation (active: $F_{(1,34)} = 3.23$, $p = 0.08$; inactive: $F_{(1,34)} = 2.33$, $p = 0.14$; omission: $F_{(1,34)} = 0.80$, $p = 0.38$; Figure 6E, top). This suggests that a drug-free period does not fundamentally change the behavioral consequences of activity in this projection.

Given that our imaging experiments revealed that activity after a lever press was correlated with animals' subsequent drug-seeking latency (Figure 5), we also asked whether optogenetic activation increased drug-seeking latency on the trial after the stimulation. We found that activation of IL-NAc neurons did in fact increase the latency to respond on the subsequent trial (2-factor mixed ANOVA with D1/D15 and stim-no stim as factors: main effect of stimulation: $F_{(1,34)} = 8.52$, $p = 0.0062$; Figure 6E, bottom). This was in contrast to latencies during stimulation, which were not altered ($F_{(1,34)} = 0.01$, $p = 0.92$; Figure 6E, top). However, activation did not affect the probability of making an active press, inactive press, or omission on the subsequent trial (active: $F_{(1,34)} = 1.76$, $p = 0.19$, inactive: $F_{(1,34)} = 0.59$, $p = 0.45$, omission: $F_{(1,34)} = 0.28$, $p = 0.60$; Figure 6E, bottom).

Finally, while rats showed a time-dependent decrease in their rate of pressing the active lever due to within-session extinction learning (2-factor repeated-measures ANOVA with stim and time as factors: main effect of time: D1 active: $F_{(5,85)} = 2.64$, $p = 0.029$; D1 inactive: $F_{(5,85)} = 1.36$, $p = 0.25$; D15 active: $F_{(5,85)} = 11.42$, $p < 0.00001$; D15 inactive: $F_{(5,85)} = 2.95$, $p = 0.017$; Figure 6F), the relative effect of stimulation on active and inactive lever pressing did not change over time (stim × time interaction: D1 active: $F_{(5,85)} = 1.08$, $p = 0.38$; D1 inactive: $F_{(5,85)} = 0.12$, $p = 0.99$; D15 active: $F_{(5,85)} = 0.55$, $p = 0.74$; D15 inactive: $F_{(5,85)} = 1.04$, $p = 0.40$). Therefore, activation of this projection seems to transiently alter the motivation to engage in drug seeking without influencing the rate of ongoing extinction learning.

To control for nonspecific effects of our optogenetic manipulation, we confirmed that stimulation had no effect in YFP control rats (2-factor mixed ANOVA with D1/D15 and stim-no stim as factors: main effect of stimulation: active: $F_{(5,19)} = 0.11$, $p = 0.74$; inactive: $F_{(1,19)} = 0.01$, $p = 0.94$: omission: $F_{(1,19)} = 0.03$, $p = 0.87$; Figure S5B) and that there was the expected interaction between the ChR2 and YFP groups with stimulation (2-factor mixed ANOVA with ChR2/YFP and stim-no stim as factors: group × stim interaction: active: $F_{(1,55)} = 9.50$, $p = 0.0032$; inactive: $F_{(1,55)} = 4.47$, $p = 0.039$; subsequent trial response latency: $F_{(1,55)} = 5.77$, $p = 0.020$; Figure S5E).

DISCUSSION

Our goal was to determine whether and how IL-NAc neurons contribute to the increase in cocaine motivation that results from a drug-free period. More specifically, we sought to identify coding properties of IL-NAc neurons during a drug-seeking test and examine how these properties are affected by a drug-free period. We found that (1) IL-NAc neurons are spatially selective in the cocaine-associated context (Figure 3), (2) across the population, IL-NAc activity decreases before the drug-seeking action (lever press; Figure 4), and (3) there is an inverse relationship between activity after the drug-seeking action and cocaine motivation on the subsequent trial (Figure 5). All of these properties

(H) Mean ± SEM activity (peak normalized) of all significant time-locked neurons (EXT and INH) in the D1 (n = 39) and D15 (n = 69) groups as well as randomly shifted data for these neurons (mean ± 2 SD; 1,000 shifted iterations). Both groups showed a decrease in activity around the time of active lever press, but the inhibition was significantly greater for the D1 group before the active lever press. *$p < 0.05$, real data compared to null distribution of shifted data. †$p < 0.05$, ‡$p < 0.01$, simple main effect of D1 versus D15.

(I) A similar pattern was observed when all recorded neurons (D1: n = 182; D15: n = 234; mean ± SEM *Z*-scored activity) were included in the analysis.

*$p < 0.05$, real data compared to null distribution of shifted data. †$p < 0.05$, simple main effect D1 versus D15.

See also Figure S3.

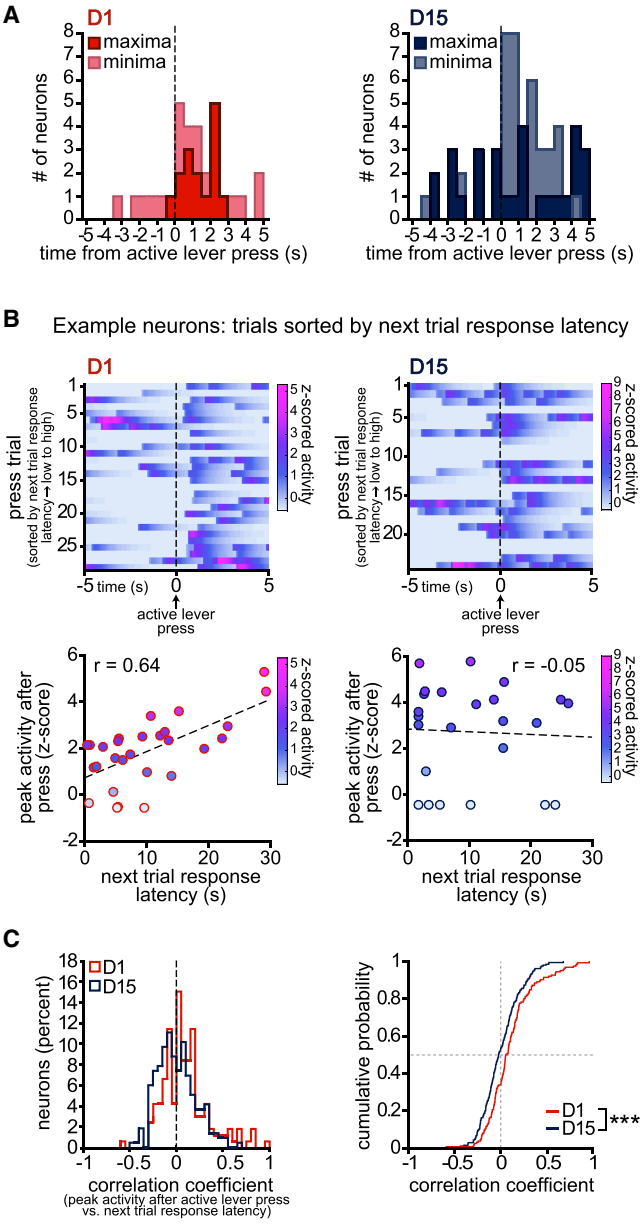

Figure 5. After the Drug-Seeking Behavior (Active Lever Press), Neural Activity Is Inversely Correlated with Motivation to Drug Seek on the Subsequent Trial, although This Relationship Is Disrupted by a Drug-free Period

(A) Most maxima and minima of neurons with significant time-locked activity occurred after the active lever press. Histograms of time of maxima (for EXT responses; D1: n = 15, D15: n = 29) and minima (for INH responses; D1: n = 26, D15: n = 40) relative to active lever press in D1 (left) and D15 (right).

(B) Top: *Z*-scored activity for all active lever presses for representative neurons in the D1 (left) and D15 (right) groups (dotted line is time of active press). Trials (vertical axis) are sorted by the response latency on the subsequent trial (longest latency on bottom). Bottom: scatterplots of peak activity (in 5 s after a press) versus next trial response latency. In the D1 example (left), higher peak activity was correlated with longer response latencies. In the D15 example (right), there was no relationship between peak activity and next trial response latency. Correlation coefficients (r) for the example neurons indicate trial-by-trial correlation between peak *Z*-scored activity in the 5 s immediately after an active lever press and latency to press on the next trial.

(C) Histogram and cumulative density function of correlation coefficients for D1 versus D15 neurons.

***p < 0.001, K-S test D1 compared to D15.

See also Figure S4.

are reduced by a longer drug-free period. In contrast to these changes in neural activity as a result of the drug-free period, optogenetic activation revealed that the *ability* of these neurons to suppress drug seeking was not significantly affected by a longer drug-free period. Together, this implies that a drug-free period may enhance cocaine motivation in part by reducing the representation of the drug-related context or drug-seeking behavior in IL-NAc neurons, or through a more general reduction in spontaneous activity (Figure 2L), without decreasing the neurons' ability to inhibit drug seeking.

Some Neural Correlates of Behavior in IL-NAc Neurons Are Consistent with a "Stop" Signal

Previous manipulations of IL or NAc activity had led to the hypothesis that IL-NAc neurons provide a "stop" on drug seeking (Augur et al., 2016; Gutman et al., 2017; Ma et al., 2014; Moorman et al., 2015; Peters et al., 2008) or other behaviors (Chudasama et al., 2003; Risterucci et al., 2003). However, neural correlates of behavior within IL-NAc projection neurons had not previously been recorded, so it was not known whether the endogenous activity was consistent with the idea that these neurons provide such a signal.

Interestingly, some of the neural correlates of drug seeking we discovered are in fact consistent with the view that IL-NAc activity serves as a "stop" signal for drug seeking, in that activity appears to be inversely related to initiating an active lever press response. For example, more neurons in the IL-NAc time-locked population are inhibited prior to the drug-seeking action (lever press) than excited, and there is an overall decrease in activity across the population before the rats press the active lever. Given the sparse activity of cortical neurons (and consequently, the infrequent calcium transient rate), it is somewhat surprising that with a calcium indicator it is possible to detect an overall decrease in spontaneous activity before the lever press. For this reason, the inhibition we report is likely an underestimate of the true inhibition in the firing rates of these neurons.

In addition to the decrease in activity immediately preceding the drug-seeking action (active lever press), we also observed an inverse relationship between activity immediately after the lever press and drug seeking on the subsequent trial. This effect is on a much longer timescale than the decrease in activity immediately preceding the lever press (2–3 s for the decrease in activity immediately preceding the lever press, versus ~30 s for the average time between trials). This suggests that neural activity is inversely related to drug seeking on multiple timescales and may indeed serve as a "stop" signal that suppresses responding.

In further support of a "stop" signal, we found that activity was higher at the start of trials on which rats omitted a press (omission trials) than at the start of trials on which animals made an active lever press. These data suggest that IL-NAc activity may serve to inhibit a motor response. However, omission data are

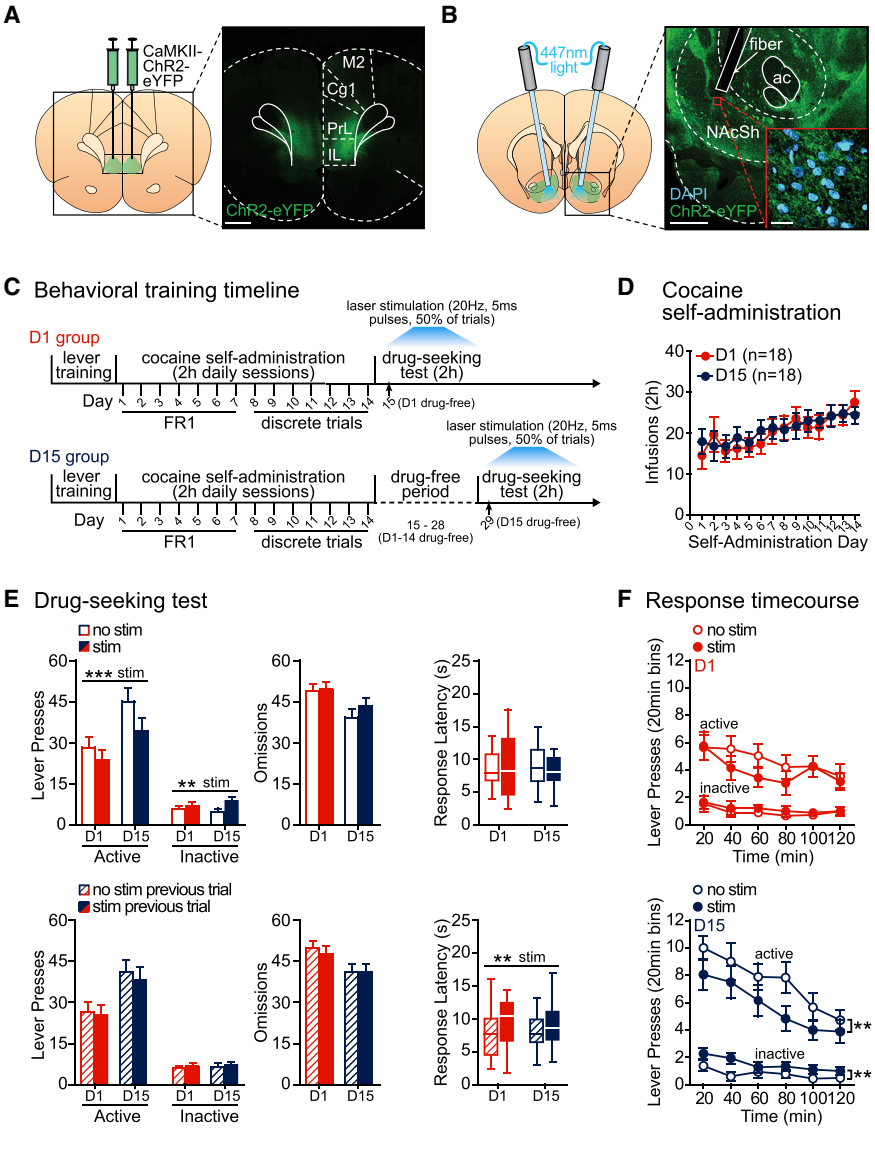

Figure 6. Activation of IL-NAc Neurons Decreases Drug-Seeking Behavior, Regardless of the Drug-free Period

(A) Left: schematic of AAV5 CaMKIIa-ChR2-YFP injection in the IL. Right: histology of ChR2 expression in the IL. M2, secondary motor cortex; Cg1, cingulate cortex; PrL, prelimbic cortex; IL, infralimbic cortex. Scale bar, 1mm.

(B) Left: schematic of fiber placement in the NAc shell. Right: histology of fiber placement and ChR2 terminal expression (inset). ChR2 is shown in green and DAPI is shown in blue. NAcSh, nucleus accumbens shell; ac, anterior commissure; Scale bars, 500 and 20 μm.

(C) Schematic of the experimental timeline. Training was completed as in the imaging experiment, but rats received laser stimulation (447 nm, 10 mW, 5-ms pulses at 20 Hz) on a random 50% of trials during the drug-seeking test.

(D) Over 14 days of cocaine self-administration, rats in both groups (D1: n = 18; D15: n = 18) self-administered a similar number of cocaine infusions (mean ± SEM; main effect of D1/D15 group: $F_{(1,442)} = 0.03$, $p = 0.87$).

(E) Top left: activation of IL-NAc neurons with laser stimulation decreased active lever pressing (mean ± SEM) and increased inactive lever pressing without changing omission rate in both the D1 and D15 groups. ***$p < 0.001$, **$p < 0.01$, main effect of stimulation. Top right: laser stimulation had no effect on response latency (median, box represents 25th and 75th percentiles; bars represent minimum and maximum values) in either group. Bottom left: laser stimulation on the previous trial had no effect on the number of active lever presses, inactive lever presses, or omissions. Bottom right: laser stimulation on the previous trial increased the latency to respond on the next trial in both the D1 and D15 group. **$p < 0.01$, main effect of stimulation.

(F) The effect of laser stimulation on active and inactive lever pressing (mean ± SEM) did not change over the course of the drug-seeking test in either the D1 (top) or D15 (bottom) group. **$p < 0.01$, main effect of stimulation.

See also Figures S5 and S6.

relatively challenging to interpret because the specific timing of the decision to omit is impossible to pinpoint, and it is difficult to disambiguate omission trials on which rats are actively inhibiting pressing from those on which they are not task engaged or performing some other behavior (e.g., grooming, exploration, etc.).

We also observed that a large fraction of IL-NAc neurons (about half) had spatially selective responses. This spatial selectivity may represent information about the cocaine-associated context and implies that IL-NAc neurons encode more than simply a "stop" signal. Other possible contributions of this information may include supporting contextually appropriate behaviors (Moorman and Aston-Jones, 2015), altering behavioral flexibility (Barker et al., 2013; Sweis et al., 2018), or biasing responses toward alternatives during changing reinforcement conditions. In fact, recent work (Cui et al., 2018) shows that activity in an mPFC projection to the NAc enhances strategy-switching ability in a spatial-egocentric task. In support of this idea, our optogenetic activation of these neurons lead to an increase in the number of inactive lever presses at the same time that it decreased active lever presses, suggesting that higher activity in IL-NAc neurons may cause animals to bias toward a new behavioral strategy. Thus, rather than simply inhibiting responding, the IL-NAc projection may integrate contextual information (e.g., responding on active lever no longer produces expected outcome) to promote a behaviorally advantageous response strategy (e.g., try the alternate lever or stop responding on the active lever).

Spatial and Temporal Responses in IL-NAc Neurons Are Degraded after the Longer Drug-free Period

We observed degraded spatial and temporal coding in IL-NAc neurons after the longer drug-free period. In other words, there

were fewer neurons with spatial response fields, there was less inhibition in neural activity preceding the drug-seeking action (active lever press), and activity after the lever press was no longer correlated with drug-seeking latency on the subsequent trial. These changes may be consistent with the hypofrontality observed in human cocaine users during withdrawal (Goldstein and Volkow, 2002). Given that IL-NAc activity suppresses drug seeking and that prefrontal cortex hypoactivity has been linked to compulsive cocaine seeking (Chen et al., 2013), the degraded coding properties of these neurons may be a contributor to the increased cocaine seeking observed after a drug-free period.

Relationship to Previous Recordings from IL and NAc during Drug Seeking

Previous electrophysiological recordings in the IL and NAc shell in the setting of a similar drug-seeking paradigm reported that a drug-free period did not alter the fraction of neurons in either area with time-locked responses to the active lever press (in contrast to time-locked neurons in the PL and NAc core, which increased in number) (Hollander and Carelli, 2005, 2007; West et al., 2014). Our findings from IL-NAc neurons are consistent with these results in the sense that although a drug-free period altered the pattern of neural responses, we did not observe an overall difference in the fraction of neurons with time-locked responses in the two groups (although we did observe an overall decrease in the fraction with spatially selective responses).

Our finding of less inhibition before an active lever press in the D15 compared to D1 group is somewhat surprising in light of our behavioral and optogenetic findings. Across both groups, a decrease in activity in IL-NAc neurons occurred before active lever presses (Figure 4C); however, D15 animals showed *less* decrease (Figures 4E–4I) but made *more* presses (compared to D1). However, it is important to consider that the observed data (Figure 4F) represent only the subset of trials on which animals pressed the active lever. In D1 animals, high IL-NAc activity may be sufficient to stop a press, and, therefore, only those trials with relatively low IL-NAc activity are included in the time-locked activity traces. Conversely, in D15 animals, the strengthening of a competing pro-drug-seeking signal (such as from the PL) may make high levels of IL-NAc activity insufficient for stopping a press. These higher activity trials would therefore be included in the activity traces in the D15 data.

Optogenetic Activation of IL-NAc Suppresses Drug Seeking, Regardless of the Length of the Drug-free Period

The optogenetic activations of IL-NAc neurons that we performed support previous suggestions that these neurons suppress drug seeking, in that there were fewer active lever presses on the stimulated trials. In addition, the latency to press the lever was greater on a trial that was subsequent to stimulation, which agreed with our observation that neural activity after the lever press was inversely correlated with the animal's latency to press the lever on the subsequent trial.

These effects on drug seeking were similar in the case of the short (1 day) versus long (15 day) drug-free period. This is in contrast to our imaging experiments in which a longer drug-free period decreased temporal and spatial encoding in this projection. While optogenetic stimulation is a tool for probing the downstream effects of activity in a projection (irrespective of neurons' endogenous activity), calcium recordings probe the endogenous activity of the neurons themselves. Theoretically, a drug-free period could affect cocaine motivation by altering activity in IL-NAc neurons, decreasing the effect of IL-NAc activity on downstream circuits, or both. Our findings suggest that a drug-free period reduces drug-related representations in IL-NAc neurons (Figures 2, 3, 4, and 5) without altering the neurons' ability to influence behavior when artificially activated (Figure 6). Therefore, our data are most consistent with the idea that the effect of IL-NAc neurons on downstream circuits is intact after the drug-free period, but neural activity within the IL-NAc neurons themselves is degraded.

The similar effect of stimulation in the two behavioral groups is somewhat surprising given that IL-NAc synaptic terminals are thought to be strengthened by a drug-free period (Ma et al., 2014; Pascoli et al., 2014). However, the stimulation we used was supra-physiological, and we cannot rule out the possibility that there may have been a ceiling effect in both groups.

Finally, the ability of the IL-NAc projection to support self-stimulation (Figure S6A) could potentially interact with animals' motivation for cocaine and influence their drug-seeking behavior. However, it is worth noting that IL-NAc activation is thought to be rewarding due to the release of dopamine (Stuber et al., 2011), and, based on prior work (Phillips et al., 2003; Stuber et al., 2005; Weiss et al., 2000), we would expect that an increase in dopamine levels would most likely lead to an increase, not a decrease, in drug seeking. Thus, the optogenetic effect we observed through IL-NAc stimulation—a decrease in drug seeking—appears to be in the wrong direction to be explained by the IL-NAc pathway stimulation being rewarding.

Conclusions

By performing the first selective recordings from IL-NAc neurons during drug seeking, we identified decreases in activity associated with drug seeking, and also spatially selective responses. These properties are diminished after a drug-free period, suggesting that this projection may become less engaged by behavior after a drug-free period. The disengagement of this "anti-relapse" projection may contribute to the heightened drug seeking that results from a drug-free period. However, our optogenetics experiments revealed that IL-NAc neurons remain capable of suppressing drug seeking, even after a longer drug-free period, suggesting that upregulation of activity in this projection may be a promising strategy for reducing aberrant cocaine-directed behaviors.

STAR★METHODS

Detailed methods are provided in the online version of this paper and include the following:

- KEY RESOURCES TABLE
- CONTACT FOR REAGENT AND RESOURCES SHARING
- EXPERIMENTAL MODEL AND SUBJECT DETAILS
- METHOD DETAILS
  - Surgery

- Cocaine Self-administration and Drug-seeking Test
- Cellular Resolution Calcium Imaging
- Optogenetic Activation of IL-NAc Neurons
- Histology
- Rat Codon Optimization of GCaMP

● QUANTIFICATION AND STATISTICAL ANALYSIS
- Behavioral analysis
- Calcium imaging experiment
- Optogenetic activation

● DATA AND SOFTWARE AVAILABILITY

SUPPLEMENTAL INFORMATION

Supplemental Information can be found online at https://doi.org/10.1016/j.neuron.2019.04.015.

ACKNOWLEDGMENTS

We thank the rest of the Witten lab, as well as J. Pillow, P. Singh, and S. Thiberge, for comments, advice, and support on this work. This research was funded by NYSCF, Pew, McKnight, NARSAD, and Sloan Foundation grants to I.B.W. and the NIH (5F32DA042515-02 to C.M.C.; U19 NS104648-01, DP2 DA035149-01, 1R01DAA047869-01, and 5R01MH106689-02 to I.B.W.). I.B.W. is a New York Stem Cell Foundation–Robertson Investigator.

AUTHOR CONTRIBUTIONS

C.M.C. and I.B.W. conceived the project and designed the experiments. C.M.C. and J.Y.C. performed experiments. E.A.E. provided and validated reagents. C.M.C. analyzed the data. M.M. provided technical training. C.M.C. and I.B.W. wrote the paper.

DECLARATION OF INTERESTS

The authors declare no competing interests.

Received: July 3, 2018
Revised: February 7, 2019
Accepted: April 5, 2019
Published: May 14, 2019

REFERENCES

Augur, I.F., Wyckoff, A.R., Aston-Jones, G., Kalivas, P.W., and Peters, J. (2016). Chemogenetic Activation of an Extinction Neural Circuit Reduces Cue-Induced Reinstatement of Cocaine Seeking. J. Neurosci. *36*, 10174–10180.

Barbera, G., Liang, B., Zhang, L., Gerfen, C.R., Culurciello, E., Chen, R., Li, Y., and Lin, D.T. (2016). Spatially Compact Neural Clusters in the Dorsal Striatum Encode Locomotion Relevant Information. Neuron *92*, 202–213.

Barker, J.M., Torregrossa, M.M., and Taylor, J.R. (2013). Bidirectional modulation of infralimbic dopamine D1 and D2 receptor activity regulates flexible reward seeking. Front. Neurosci. *7*, 126.

Bloodgood, D.W., Sugam, J.A., Holmes, A., and Kash, T.L. (2018). Fear extinction requires infralimbic cortex projections to the basolateral amygdala. Transl. Psychiatry *8*, 60.

Calu, D.J., Stalnaker, T.A., Franz, T.M., Singh, T., Shaham, Y., and Schoenbaum, G. (2007). Withdrawal from cocaine self-administration produces long-lasting deficits in orbitofrontal-dependent reversal learning in rats. Learn. Mem. *14*, 325–328.

Cameron, C.M., and Carelli, R.M. (2012). Cocaine abstinence alters nucleus accumbens firing dynamics during goal-directed behaviors for cocaine and sucrose. Eur. J. Neurosci. *35*, 940–951.

Carelli, R.M., Ijames, S.G., and Crumling, A.J. (2000). Evidence that separate neural circuits in the nucleus accumbens encode cocaine versus "natural" (water and food) reward. J. Neurosci. *20*, 4255–4266.

Chang, J.Y., Janak, P.H., and Woodward, D.J. (2000). Neuronal and behavioral correlations in the medial prefrontal cortex and nucleus accumbens during cocaine self-administration by rats. Neuroscience *99*, 433–443.

Chen, B.T., Yau, H.J., Hatch, C., Kusumoto-Yoshida, I., Cho, S.L., Hopf, F.W., and Bonci, A. (2013). Rescuing cocaine-induced prefrontal cortex hypoactivity prevents compulsive cocaine seeking. Nature *496*, 359–362.

Chudasama, Y., Passetti, F., Rhodes, S.E., Lopian, D., Desai, A., and Robbins, T.W. (2003). Dissociable aspects of performance on the 5-choice serial reaction time task following lesions of the dorsal anterior cingulate, infralimbic and orbitofrontal cortex in the rat: differential effects on selectivity, impulsivity and compulsivity. Behav. Brain Res. *146*, 105–119.

Conrad, K.L., Tseng, K.Y., Uejima, J.L., Reimers, J.M., Heng, L.J., Shaham, Y., Marinelli, M., and Wolf, M.E. (2008). Formation of accumbens GluR2-lacking AMPA receptors mediates incubation of cocaine craving. Nature *454*, 118–121.

Cui, Q., Li, Q., Geng, H., Chen, L., Ip, N.Y., Ke, Y., and Yung, W.H. (2018). Dopamine receptors mediate strategy abandoning via modulation of a specific prelimbic cortex-nucleus accumbens pathway in mice. Proc. Natl. Acad. Sci. USA *115*, E4890–E4899.

De Biasi, M., and Dani, J.A. (2011). Reward, addiction, withdrawal to nicotine. Annu. Rev. Neurosci. *34*, 105–130.

Gawin, F.H. (1991). Cocaine addiction: psychology and neurophysiology. Science *251*, 1580–1586.

Goldstein, R.Z., and Volkow, N.D. (2002). Drug addiction and its underlying neurobiological basis: neuroimaging evidence for the involvement of the frontal cortex. Am. J. Psychiatry *159*, 1642–1652.

Grimm, J.W., Hope, B.T., Wise, R.A., and Shaham, Y. (2001). Neuroadaptation. Incubation of cocaine craving after withdrawal. Nature *412*, 141–142.

Gutman, A.L., Nett, K.E., Cosme, C.V., Worth, W.R., Gupta, S.C., Wemmie, J.A., and LaLumiere, R.T. (2017). Extinction of Cocaine Seeking Requires a Window of Infralimbic Pyramidal Neuron Activity after Unreinforced Lever Presses. J. Neurosci. *37*, 6075–6086.

Hollander, J.A., and Carelli, R.M. (2005). Abstinence from cocaine self-administration heightens neural encoding of goal-directed behaviors in the accumbens. Neuropsychopharmacology *30*, 1464–1474.

Hollander, J.A., and Carelli, R.M. (2007). Cocaine-associated stimuli increase cocaine seeking and activate accumbens core neurons after abstinence. J. Neurosci. *27*, 3535–3539.

Hwa, L., Besheer, J., and Kash, T. (2017). Glutamate plasticity woven through the progression to alcohol use disorder: a multi-circuit perspective. F1000Res. *6*, 298.

Janak, P.H., Chang, J.-Y., and Woodward, D.J. (1999). Neuronal spike activity in the nucleus accumbens of behaving rats during ethanol self-administration. Brain Res. *817*, 172–184.

Kalivas, P.W., and Volkow, N.D. (2011). New medications for drug addiction hiding in glutamatergic neuroplasticity. Mol. Psychiatry *16*, 974–986.

Koya, E., Cruz, F.C., Ator, R., Golden, S.A., Hoffman, A.F., Lupica, C.R., and Hope, B.T. (2012). Silent synapses in selectively activated nucleus accumbens neurons following cocaine sensitization. Nat. Neurosci. *15*, 1556–1562.

Lee, J., Finkelstein, J., Choi, J.Y., and Witten, I.B. (2016). Linking Cholinergic Interneurons, Synaptic Plasticity, and Behavior during the Extinction of a Cocaine-Context Association. Neuron *90*, 1071–1085.

Ma, Y.-Y., Lee, B.R., Wang, X., Guo, C., Liu, L., Cui, R., Lan, Y., Balcita-Pedicino, J.J., Wolf, M.E., Sesack, S.R., et al. (2014). Bidirectional modulation of incubation of cocaine craving by silent synapse-based remodeling of prefrontal cortex to accumbens projections. Neuron *83*, 1453–1467.

Ma, T., Cheng, Y., Roltsch Hellard, E., Wang, X., Lu, J., Gao, X., Huang, C.C.Y., Wei, X.Y., Ji, J.Y., and Wang, J. (2018). Bidirectional and long-lasting control of alcohol-seeking behavior by corticostriatal LTP and LTD. Nat. Neurosci. *21*, 373–383.

McGlinchey, E.M., James, M.H., Mahler, S.V., Pantazis, C., and Aston-Jones, G. (2016). Prelimbic to Accumbens Core Pathway Is Recruited in a Dopamine-Dependent Manner to Drive Cued Reinstatement of Cocaine Seeking. J. Neurosci. *36*, 8700–8711.

Moorman, D.E., and Aston-Jones, G. (2015). Prefrontal neurons encode context-based response execution and inhibition in reward seeking and extinction. Proc. Natl. Acad. Sci. USA *112*, 9472–9477.

Moorman, D.E., James, M.H., McGlinchey, E.M., and Aston-Jones, G. (2015). Differential roles of medial prefrontal subregions in the regulation of drug seeking. Brain Res. *1628*, 130–146.

Murugan, M., Jang, H.J., Park, M., Miller, E.M., Cox, J., Taliaferro, J.P., Parker, N.F., Bhave, V., Hur, H., Liang, Y., et al. (2017). Combined Social and Spatial Coding in a Descending Projection from the Prefrontal Cortex. Cell *171*, 1663–1677.e16.

Otis, J.M., Namboodiri, V.M., Matan, A.M., Voets, E.S., Mohorn, E.P., Kosyk, O., McHenry, J.A., Robinson, J.E., Resendez, S.L., Rossi, M.A., and Stuber, G.D. (2017). Prefrontal cortex output circuits guide reward seeking through divergent cue encoding. Nature *543*, 103–107.

Park, M., Weller, J.P., Horwitz, G.D., and Pillow, J.W. (2014). Bayesian active learning of neural firing rate maps with transformed gaussian process priors. Neural Comput. *26*, 1519–1541.

Pascoli, V., Terrier, J., Espallergues, J., Valjent, E., O'Connor, E.C., and Lüscher, C. (2014). Contrasting forms of cocaine-evoked plasticity control components of relapse. Nature *509*, 459–464.

Peters, J., LaLumiere, R.T., and Kalivas, P.W. (2008). Infralimbic prefrontal cortex is responsible for inhibiting cocaine seeking in extinguished rats. J. Neurosci. *28*, 6046–6053.

Phillips, P.E.M., Stuber, G.D., Heien, M.L.A.V., Wightman, R.M., and Carelli, R.M. (2003). Subsecond dopamine release promotes cocaine seeking. Nature *422*, 614–618.

Pinto, L., and Dan, Y. (2015). Cell-Type-Specific Activity in Prefrontal Cortex during Goal-Directed Behavior. Neuron *87*, 437–450.

Risterucci, C., Terramorsi, D., Nieoullon, A., and Amalric, M. (2003). Excitotoxic lesions of the prelimbic-infralimbic areas of the rodent prefrontal cortex disrupt motor preparatory processes. Eur. J. Neurosci. *17*, 1498–1508.

Robbins, T.W., Everitt, B.J., and Nutt, D.J. (2010). The Neurobiology of Addiction: New Vistas (Oxford University Press).

Robledo, P., and Koob, G.F. (1993). Two discrete nucleus accumbens projection areas differentially mediate cocaine self-administration in the rat. Behav. Brain Res. *55*, 159–166.

Saunders, B.T., Yager, L.M., and Robinson, T.E. (2013). Cue-evoked cocaine "craving": role of dopamine in the accumbens core. J. Neurosci. *33*, 13989–14000.

Siciliano, C.A., and Tye, K.M. (2019). Leveraging calcium imaging to illuminate circuit dysfunction in addiction. Alcohol *74*, 47–63.

Spellman, T., Rigotti, M., Ahmari, S.E., Fusi, S., Gogos, J.A., and Gordon, J.A. (2015). Hippocampal-prefrontal input supports spatial encoding in working memory. Nature *522*, 309–314.

Stuber, G.D., Wightman, R.M., and Carelli, R.M. (2005). Extinction of cocaine self-administration reveals functionally and temporally distinct dopaminergic signals in the nucleus accumbens. Neuron *46*, 661–669.

Stuber, G.D., Sparta, D.R., Stamatakis, A.M., van Leeuwen, W.A., Hardjoprajitno, J.E., Cho, S., Tye, K.M., Kempadoo, K.A., Zhang, F., Deisseroth, K., and Bonci, A. (2011). Excitatory transmission from the amygdala to nucleus accumbens facilitates reward seeking. Nature *475*, 377–380.

Sun, W.-L., Coleman, N.T., Zelek-Molik, A., Barry, S.M., Whitfield, T.W., Jr., and McGinty, J.F. (2014). Relapse to cocaine-seeking after abstinence is regulated by cAMP-dependent protein kinase A in the prefrontal cortex. Addict. Biol. *19*, 77–86.

Sweis, B.M., Larson, E.B., Redish, A.D., and Thomas, M.J. (2018). Altering gain of the infralimbic-to-accumbens shell circuit alters economically dissociable decision-making algorithms. Proc. Natl. Acad. Sci. USA *115*, E6347–E6355.

Tran-Nguyen, L.T., Fuchs, R.A., Coffey, G.P., Baker, D.A., O'Dell, L.E., and Neisewander, J.L. (1998). Time-dependent changes in cocaine-seeking behavior and extracellular dopamine levels in the amygdala during cocaine withdrawal. Neuropsychopharmacology *19*, 48–59.

Walker, D.M., Cates, H.M., Loh, Y.E., Purushothaman, I., Ramakrishnan, A., Cahill, K.M., Lardner, C.K., Godino, A., Kronman, H.G., Rabkin, J., et al. (2018). Cocaine Self-administration Alters Transcriptome-wide Responses in the Brain's Reward Circuitry. Biol. Psychiatry *84*, 867–880.

Wang, Q., Yang, S.-T., and Li, B.-M. (2015). Neuronal representation of audio-place associations in the medial prefrontal cortex of rats. Mol. Brain *8*, 56.

Wang, J., Ishikawa, M., Yang, Y., Otaka, M., Kim, J.Y., Gardner, G.R., Stefanik, M.T., Milovanovic, M., Huang, Y.H., Hell, J.W., et al. (2018). Cascades of Homeostatic Dysregulation Promote Incubation of Cocaine Craving. J. Neurosci. *38*, 4316–4328.

Warden, M.R., Selimbeyoglu, A., Mirzabekov, J.J., Lo, M., Thompson, K.R., Kim, S.Y., Adhikari, A., Tye, K.M., Frank, L.M., and Deisseroth, K. (2012). A prefrontal cortex-brainstem neuronal projection that controls response to behavioural challenge. Nature *492*, 428–432.

Weiss, F., Maldonado-Vlaar, C.S., Parsons, L.H., Kerr, T.M., Smith, D.L., and Ben-Shahar, O. (2000). Control of cocaine-seeking behavior by drug-associated stimuli in rats: effects on recovery of extinguished operant-responding and extracellular dopamine levels in amygdala and nucleus accumbens. Proc. Natl. Acad. Sci. USA *97*, 4321–4326.

West, E.A., Saddoris, M.P., Kerfoot, E.C., and Carelli, R.M. (2014). Prelimbic and infralimbic cortical regions differentially encode cocaine-associated stimuli and cocaine-seeking before and following abstinence. Eur. J. Neurosci. *39*, 1891–1902.

Xia, L., Nygard, S.K., Sobczak, G.G., Hourguettes, N.J., and Bruchas, M.R. (2017). Dorsal-CA1 Hippocampal Neuronal Ensembles Encode Nicotine-Reward Contextual Associations. Cell Rep. *19*, 2143–2156.

Zhou, P., Resendez, S.L., Rodriguez-Romaguera, J., Jimenez, J.C., Neufeld, S.Q., Giovannucci, A., Friedrich, J., Pnevmatikakis, E.A., Stuber, G.D., Hen, R., et al. (2018). Efficient and accurate extraction of in vivo calcium signals from microendoscopic video data. eLife *7*, e28728.

Ziv, Y., Burns, L.D., Cocker, E.D., Hamel, E.O., Ghosh, K.K., Kitch, L.J., El Gamal, A., and Schnitzer, M.J. (2013). Long-term dynamics of CA1 hippocampal place codes. Nat. Neurosci. *16*, 264–266.

STAR★METHODS

KEY RESOURCES TABLE

REAGENT or RESOURCE	SOURCE	IDENTIFIER
Antibodies		
mouse monoclonal anti-GFP	Life Technologies Corporation	G10362
donkey anti-rabbit conjugated to AlexaFlour 488	Jackson ImmunoResearch	711-545-152; RRID:AB_2313584
mouse monoclonal anti-beta-actin	Sigma	A1978; RRID:AB_476692
rabbit polyclonal anti-GFP	Thermo Fisher	A-11122; RRID:AB_221569
Bacterial and Virus Strains		
CAV-Cre virus	IGMM Vector core, France	N/A
AAV2/5-CAG-DIO-GCamp6f-WPRE-SV40	UPenn Vector Core	AV-5-PV2816 https://www.addgene.org/100835/
AAV2/5-CAG-DIO-RatOptimized-GCamp6f-WPRE-SV40	PNI Viral Core, Princeton	AAV-VC58
AAV2/5-CamKII-hChR2(H134R)-eYFP	UNC Vector Core	https://www.addgene.org/26969/
AAV2/5-CamKII-hChR2(H134R)-eYFP	UPenn Vector Core	https://www.addgene.org/26969/
AAV2/5-CamKIIa-eYFP	UNC Vector Core	http://www.everyvector.com/sequences/show_public/11037
Experimental Models: Organisms/Strains		
rat: wild-type Long Evans	Charles River	006
Rattus norvegicus fibroblast	ATCC	CRL-1764
Software and Algorithms		
spatial estimation using GP regression	Murugan et al., 2017	https://github.com/wittenlab/Spatial-field-estimates-Murugan-et-al-Cell-2017#gp-regression-for-place-field-estimation
Other		
fibers for optogenetics	Thor labs	BFL37-300
ferrules for optogenetics	Precision Fiber Products	MM-FER-2006SS- 3300
GRIN lens, 0.5 mm diameter, ~8.4 mm length	Inscopix	130-000152
GRIN lens, 0.6 mm diameter, ~7.3 mm length	Inscopix	130-000150
prism probe GRIN lens, 1.0mm diameter, ~9.1 mm length	Inscopix	130-000444
imaging baseplate	Inscopix	100-000279
baseplate cover	Inscopix	100-000241

CONTACT FOR REAGENT AND RESOURCES SHARING

Further information and requests for resources and reagents should be directed to and will be fulfilled by the Lead Contact, Ilana B. Witten (iwitten@princeton.edu).

EXPERIMENTAL MODEL AND SUBJECT DETAILS

All procedures were conducted in accordance with the National Institutes of Health Guidelines for the Care and Use of Laboratory Animals and were approved by the Princeton University Institutional Animal Care and Use Committee (IACUC). For all experiments, male wild-type Long Evans rats (Charles River: 006; n = 90) aged 8 weeks (~275-325 g) upon arrival were used. Rats were housed individually and maintained on a reverse 12-h light:dark cycle (lights off at 8:00 a.m.). All behavioral testing was performed during the dark phase of the cycle. Food and water were available *ad libitum* for the ~7-day period of acclimation to the vivarium and during

recovery from all surgical procedures. During behavioral training and drug-free period, animals were restricted to no < 85% of their preoperative body weight by limiting food access to ~19 g per day.

METHOD DETAILS

Surgery

For all surgical procedures, rats were anesthetized with ketamine and xylazine (100 mg/kg and 7 mg/kg, respectively, i.p.) and the anesthetic plane maintained with isoflurane (1%–2%). Rats received the antibiotic enrofloxacin (5 mg/kg, i.m.) before surgery and the analgesic meloxicam (2 mg/kg, s.c.) before and 24 h after surgery. Rats were allowed a 5- to 7-day recovery period following all surgeries.

Calcium imaging

Rats (n = 33; aged 8-9 weeks) were placed in a small animal stereotax (Kopf Instruments, Tujunga, CA, USA) and unilaterally injected in the NAc (ML +1.0 mm, AP +1.7 mm relative to bregma, DV −7.4 mm relative to skull) with a retrogradely transporting CAV2-Cre virus (n = 33 rats, 1 μl, titer 2.5 × 10^{12} parts/ml, IGMM Vector core, France) and in the IL (ML +0.6 mm, AP +3.1 mm relative to bregma, DV −5.5 & −4.7 mm relative to skull) with AAV2/5-CAG-DIO-GCamp6f-WPRE-SV40 (n = 29 rats, 2 μl, titer 1.17 × 10^{13} parts/ml, UPenn Vector Core) or AAV2/5-CAG-DIO-RatOptimized-GCamp6f-WPRE-SV40 (see Rat Codon Optimization of GCaMP below; n = 4 rats, 2 μl, titer 1.15 × 10^{13} parts/ml, Princeton Vector Core). One week later, rats were implanted with a GRIN lens (n = 32 rats, 0.5-0.6 mm in diameter, 7.3-8.4 mm in length; Inscopix, Palo Alto, CA, USA, 130-000152, 130-000150) or GRIN lens with prism attached (n = 1 rat, 1mm in diameter, 9.1 mm in length, 1mm x 1mm prism; Inscopix, Palo Alto, CA, USA, 130-000444) in the IL (ML +0.9 mm, AP +2.6 mm relative to bregma, DV −4.4 to −4.7 mm relative to skull). The lens was secured with metabond (Parkell, Edgewood, NY, USA) and fixed to the skull with skull screws and dental cement (Lang Dental, Wheeling, IL, USA). A plastic cap was glued in place to protect the lens. Rats were also implanted with an intravenous catheter using established procedures (Carelli et al., 2000). Briefly, a custom-made catheter (Access Technologies and Norfolk Medical, Skokie, IL, USA) was inserted into the right jugular vein and passed subcutaneously to the back of the animal between the shoulder blades. During the recovery period, catheters were flushed daily with heparin (1USP unit/ml) dissolved in 0.9% sterile saline (0.1ml, i.v.). Two to three weeks after lens and catheter implantation, a baseplate (Inscopix, Palo Alto, CA, USA, 100-000279) which supported attachment of a miniaturized microscope (epi-fluorescence, 475 nm LED; Inscopix, Palo Alto, CA, USA) was cemented in place above the GRIN lens. A baseplate cover (Inscopix, Palo Alto, CA, USA, 100-000241) was attached to protect the lens. Some rats (n = 11) did not have any recorded neurons and were included only in behavioral analysis (Figure 1). Of rats included in imaging analysis (n = 22), 2 were implanted in the left hemisphere and 20 were implanted in the right hemisphere.

Optogenetic terminal activation

Rats (n = 57; aged 8-9 weeks) were placed in a stereotax and bilaterally injected in the IL (ML ± 0.6 mm, AP +3.1 mm relative to bregma, DV −5.6 & −4.8 mm relative to skull) with either AAV2/5-CamKII-hChR2(H134R)-eYFP (n = 29 rats, 2 μL per hemisphere, titer 4 × 10^{12} parts/ml, UNC vector core; n = 7 rats, 2 μL per hemisphere, 9.6 × 10^{13} titer parts/ml, UPenn vector core) or AAV2/5-CamKIIa-eYFP (n = 21 rats, 2 μL per hemisphere, titer 7.5 × 10^{12} parts/ml, UNC vector core). ChR2-YFP is thought to diffuse passively to axon terminals, and previous work indicates that a 3-4 month time frame is appropriate for terminal expression in rats, given the length of long-range axons in this species (Warden et al., 2012). Therefore, optical fibers and catheters were implanted during a second surgery performed 3-4 months after virus injection. Optical fibers (300 μm core diameter, 0.37 NA; Thor Labs, BFL37-300) attached to stainless steel ferrules (PFP, Milpitas, CA, USA, MM-FER-2006SS-3300) were implanted bilaterally above the NAc shell (ML ± 2.46 mm, AP +1.8 mm relative to bregma, DV −7.08 mm relative to skull, 10° angle).

Cocaine Self-administration and Drug-seeking Test

Rats were placed on food restriction (~19 g of food per day) for 24 h before training began, and food restriction was maintained for the duration of the study. All behavioral experiments were performed in a modular operant chamber (Med. Associates Inc., St. Albans, VT, USA; 30.5 × 24.1 × 21 cm, ENV-008CT, for optogenetic experiments, or 30.5 × 24.1 × 29.2 cm, ENV-007CT, for imaging experiments) housed within a sound-attenuating chamber (Med Associates; ENV-018V). Two retractable levers and a central reward receptacle were confined to one wall of the chamber, and a houselight and speaker were located on the opposite side of the chamber. A computer-controlled syringe pump was located outside the sound-attenuating chamber.

Rats first underwent 5 days of lever training. The first day consisted of habituation to the chamber with non-contingent delivery of 20% sweetened condensed milk (0.05ml/reward, 50-60 rewards; 20 min session) to the reward receptacle. Rats were then trained to lever press for milk delivery on a fixed ratio 1 (FR1) schedule of reinforcement for 4 days (30 min sessions). A response on the active lever delivered 0.05ml milk; a response on the inactive lever had no programmed consequence. On the last day of lever training, an active lever press also resulted in lever retraction for 20 s in addition to milk delivery. This training schedule allowed rats to acclimate to lever pressing and lever retraction before beginning cocaine self-administration.

Rats then underwent daily 2 h cocaine self-administration sessions for 14 consecutive days. The first 7 days of self-administration training were performed under an FR1 schedule of reinforcement in which an active lever press resulted in cocaine infusion (0.33mg/0.2ml/inf, ~1mg/kg; 6 s) paired with a tone/houselight conditioned stimulus (CS; 20 s) and lever retraction (20 s). Inactive lever presses had no programmed consequence. The last 7 days of training consisted of a modified FR1 schedule with discrete trials

(Figure 1B). The start of each trial was signaled by extension of the levers into the chamber, and rats could perform 1 of 3 responses: active lever press, inactive lever press, or omission. Active lever presses resulted in cocaine infusion (6 s), CS presentation (20 s), and lever retraction (20 s). Inactive lever presses resulted in lever retraction and a variable inter-trial interval (ITI; 15-30 s). Omissions occurred if a rat made no response for 30 s and resulted in lever retraction and a variable ITI (15-30 s).

Following completion of cocaine self-administration, rats were divided into 2 groups: the D1 group underwent a 1-day drug-free period (equivalent to the normal ~24h drug-free period that elapses between daily self-administration sessions), and the D15 group underwent a 15-day drug-free period. During the drug-free period, rats remained in their homecage without access to cocaine. After this period, all rats underwent a single test of cue-induced drug-seeking to assess cocaine motivation. This test was identical to the discrete trials self-administration paradigm described above except that an active lever press resulted in CS presentation and lever retraction but no drug delivery. The number of active lever presses rats make under these conditions is the operational measure of cocaine motivation. For the imaging experiment, CS probes (5 s non-contingent presentation of the tone/houselight stimulus previously paired with cocaine delivery) were also given during a randomly selected subset of ITIs (average of 11 probes per session).

Cellular Resolution Calcium Imaging

During cocaine self-administration training, rats were acclimated to being tethered by attaching a commutating spring to a "dummy" ferrule cemented to the headcap formed around the baseplate. This mimicked the tether of the miniaturized microscope used during test days. Rats were also habituated by attaching the microscope to the baseplate at least twice prior to testing. Before the start of a drug-seeking test, the miniaturized microscope was attached to the baseplate of awake, unrestrained rats and locked in place with a set screw. During the drug-seeking test (1h), the LED power was maintained at 20 to 30% and the analog gain on the image sensor was set to 1.5. Grayscale tiff images were collected at 10 frames per second using Inscopix nVista *HD* software (Inscopix, Palo Alto, CA). Coincident with each frame, a signal was sent to a digital signal processor (RZ5D, TDT, Alachua, FL, USA), allowing neural data to be time-stamped and synchronized with behavioral events. Another computer controlled the behavioral events of the experiment (Med Associates Inc., St. Albans, VT, USA) and sent digital outputs corresponding to each event to the digital signal processor. Additionally, head tracking data was obtained by using the TDT RV2 system linked to a camera (frame rate 101.7254 Hz) directly above the operant chamber. The RV2 system was trained to detect the blue LED on the miniaturized microscope mounted on rats' heads. Shape-preserving piecewise cubic interpolation (*pchip* function in MATLAB) was used to fill in gaps in tracking for any periods when the LED signal was lost. Finally, position data were downsampled to 10 Hz to match the acquisition rate of neural data.

Extraction of activity traces

Imaging data was spatially downsampled by a factor of 4 and motion corrected with Mosaic software (Inscopix, Palo Alto, CA, USA). The motion correction used a translational correction algorithm based on cross-correlations computed on consecutive frames (motion correction parameters were as follows, motion correction type: translation only; reference image: the mean image; speed/accuracy balance: 0.1; subtract spatial mean [r = 20 pixels], invert, and apply spatial mean [r = 5 pixels]). Custom MATLAB (Mathworks, Natick, MA) scripts were then used for all subsequent imaging data analysis. After motion correction, a CNMFe algorithm (Zhou et al., 2018) was used to identify individual neurons, obtain their fluorescence traces, and deconvolve the fluorescence signal into firing rate estimates. Fluorescence traces were used for time-locked analysis (see below). Inferred firing rates (based on the CNMFe algorithm) were used for spatial receptive field estimates (see below).

Optogenetic Activation of IL-NAc Neurons

At the start of the behavioral test session, ferrules were connected to patch cables via ceramic sleeves. Patch cables were protected with a metal spring and attached to a bilateral optical commutator (Doric Lenses, Quebec, Canada). The commutator was linked to a laser (100 mW, 447 nm, OEM Laser Systems, Draper, UT, USA) with a multimode fiber coupler for an FC/PC connection. Laser output was calibrated to ~10 mW measured at the tip of the fiber. Rats were habituated to this set-up by attaching ferrules to "dummy" patch cables that were not connected to a laser during all cocaine self-administration sessions. During the drug-seeking test (2 h), laser stimulation (20 Hz, 5 ms pulses) was presented on a random 50% of trials. On stimulation trials, laser onset began at trial start (lever extension) and stimulation lasted for the duration of the trial, including the response (active lever press, inactive lever press, or omission) and subsequent outcome (CS or ITI).

The day after the drug-seeking test, all rats underwent a single 4 h test for intracranial self-stimulation (ICSS). This test was performed in the same operant chambers used for self-administration training and the drug-seeking test; however, rats were assigned to a different specific chamber for the ICSS test. A nosepoke at an active hole resulted in 5 s of stimulation (~10 mW, 20 Hz, 5 ms pulses) followed by a 1 s timeout. Rats could continue to nosepoke during the stimulation and timeout periods. These nosepokes were recorded but did not result in additional stimulation presentations. A nosepoke at an inactive hole had no programmed consequence.

Finally, rats were tested for possible non-specific locomotor effects of optogenetic stimulation in a locomotor chamber (52 × 52 × 52 cm). Rats were allowed to explore the locomotor chamber for 3 min with no laser stimulation, followed by 3 min of laser light stimulation (~10 mW, 20 Hz, 5 ms pulses), and terminating with an additional 3 min of no light. The location and velocity of rats was tracked using Ethovision (Nodulus). Note that only a subset of rats that performed the drug-seeking and ICSS tests also underwent locomotor testing (ChR2 group, n = 17; YFP group, n = 6). An additional 11 YFP control rats were used for locomotor testing but not the drug-seeking/ICSS test.

Histology

Rats were deeply anesthetized with pentobarbital sodium (2 mg/kg, i.p.) and transcardially perfused with 1x phosphate-buffered saline (PBS), followed by fixation with 4% paraformaldehyde (PFA) in PBS. Brains were dissected out and post-fixed in 4% PFA overnight before being transferred to 30% sucrose in PBS solution. 40 μm thick coronal sections containing the brain regions of interest were cut on a freezing microtome or cryostat.

For immunohistochemistry, slices were blocked in 3% normal donkey serum (NDS) in PBS with 0.25% Triton X-100 for 1 h. Sections were then incubated at 4°C overnight in monoclonal rabbit anti-GFP primary antibody (1:1000, Life Technologies, No. G10362). PBS washes were performed to remove primary antibody, and slices were then incubated for 2 h in AlexaFluor488-conjugated donkey anti–rabbit IgG (1:500, Jackson ImmunoResearch, No. 711-545-152). Following PBS washes, slices were mounted in 1:2,500 DAPI in Fluoromount-G.

For the GCaMP6f imaging experiments, coronal sections of IL were imaged with a Nikon Ti2000E epifluorescence microscope to verify targeting of the GRIN lens to IL. A Leica TCS SP8 confocal microscope was used to confirm virus expression and nuclear exclusion of GCaMP6f as well as produce Figure 2C–G. 11 of 33 rats did not show GCaMP6f expression and were excluded from analysis of calcium data; however, their behavior during the drug-seeking test was included in analysis.

For the optogenetic excitation experiments, coronal sections were imaged with a Nikon Ti2000E epifluorescence microscope to confirm expression of the virus in IL cell bodies and NAc terminals, as well as optical fiber targeting to the NAc shell.

Rat Codon Optimization of GCaMP

To increase the translation efficiency of GCaMP6f in rats, we replaced 14% (188 bp out of a total of 1350bp) of the GCaMP6f nucleotide sequence to match the codon usage bias of *Rattus norvegicus*. The new 1350bp rat-Optimized-GCaMP6f gene was synthesized by GenScript (Piscataway, NJ), and cloned into an AAV plasmid replacing the standard GCaMP6f sequence to generate CAG-DIO-RatOptimized-GCaMP6f-WPRE-SV40.

To confirm a significant increase in the expression levels of the codon optimized GcaMP6f over the standard version, Rat-2 (*Rattus norvegicus* fibroblast, ATCC CRL-1764) cells were transfected with plasmid DNA corresponding to either standard GCaMP6f or rat-codon-optimized CAG-GCaMP6f for 48h, lysed, and analyzed by western blot with anti-beta-actin antibody (1:5000 dilution, Sigma A1978), and anti-GFP antibody (1:2000 dilution, Thermo Fisher A-11122). The intensity of each GCaMP6f band was normalized to the corresponding beta-actin band, to determine the intensity ratio of rat-codon-optimized GCaMP6f, over standard GCaMP6f. The average ratio from three independent western blots was 2.70 (gel #1: 2.3 gel #2: 1.96, gel #3: 3.84; determined with Fiji software (https://www.ncbi.nlm.nih.gov/pubmed/22743772; Figure S1I), indicating a significant increase in the expression levels of the codon optimized GCaMP6f over the standard version. However, we did not observe any qualitative differences in our *in vivo* imaging between this construct and the standard construct.

QUANTIFICATION AND STATISTICAL ANALYSIS

All statistical tests and data analyses were performed using MATLAB, Graphpad Prism Software, or GraphPad QuickCalcs online calculators (https://www.graphpad.com/quickcalcs/). Statistical details of experiments can be found in the results and appropriate figure legends.

Behavioral analysis

The number of active lever presses made during all 14 days of cocaine self-administration was compared between the D1 and D15 groups. A 2-factor mixed ANOVA with group (D1 or D15) as between-subjects factor and training day as within-subjects factor was used to determine significance (Figures 1C and 6D; Figures S1H, S5A, and S5D). The same analysis was also used to compare inactive lever pressing (Figure S1).

For the data in Figure 1D, two-tailed t tests comparing the number of active lever presses, inactive lever presses, and omissions made by the D1 and D15 groups during the drug-seeking test were used to determine significance. Response latency was calculated as the median time from trial start (lever extension) to lever press (active and inactive) per rat. A two-tailed t test comparing response latency in the D1 and D15 groups was used to determine significance. For all behavioral measures, a p value < 0.05 was designated as significant.

Calcium imaging experiment

For the data in Figure 2K, virus expression time was compared between animals in the D1 and D15 groups with a two-tailed t test. For the data in Figure 2L, individual transient events were determined by deconvolving the fluorescence signal into firing rate estimates using the CNMFe algorithm (Zhou et al., 2018). The inter-event interval was defined as the time between consecutive local maxima in the estimate of firing rate. Finally, the mean inter-event interval was calculated for each neuron. A K-S test comparing the cumulative density functions for D1 and D15 neurons as well as a two-tailed t test comparing the mean across all D1 and D15 neurons was used to determine significance.

Spatial selectivity

For the data in Figure 3, we first estimated spatial fields of all IL-NAc neurons and then classified a subset as displaying significant spatial selectivity. To accomplish this, we used a Bayesian approach based on a Gaussian process (GP) regression model (Park et al., 2014) adapted for calcium fluorescence imaging data. This model provides a principled statistical framework for quantifying the relationship between spatial position and neural activity and has been described in detail elsewhere (Murugan et al., 2017). The operant chamber was discretized into bins of ~1.25cm, resulting in a discrete place field map of 24 × 20 bins. To assess the significance of each neuron's spatial selectivity during the drug-seeking test, the predicted fluorescence was compared to the actual fluorescence with cross-validation (based on the spatial RF generated from the remaining 90% of data). Neurons were classified as spatially encoding if there was a significant positive correlation between the predicted and actual fluorescence (Pearson correlation coefficient, $p < 0.01$). For Figure 3D, a Fisher exact test comparing the percentage of spatial encoding neurons in the D1 and D15 groups was used to determine significance.

For the data in Figure S2A, a chi square test comparing the percentage of neurons timelocked, spatial, both, or NS in the D1 and D15 groups was used to determine significance. This test was followed by post hoc Fisher exact tests (with Bonferroni correction) to separately compare the percentage of neurons in each condition between the D1 and D15 groups. For the data in Figure S2C, we compared two models to predict each neurons' activity. The first model used the spatial field for the entire behavioral session to predict neural activity, while the second model allowed different spatial fields for different behavioral epochs (active press, inactive press, omission, or inter- trial interval). Behavioral epochs included the time from trial start to press (or lever retraction in the case of omission). Finally, we used cross-validation to compare the ability of each model to predict left-out data. For the data in Figure S2D, model fits (r value) were compared with a 2-factor mixed ANOVA with group (D1 or D15) as between-subjects factor and model type (spatial only or spatial + behavior) as within-subjects factor.

Time-locked activity

For the data in Figure 4 (and Figure S3), we first classified neurons based on whether they displayed significantly time-locked changes in neuronal activity relative to behavioral events of interest (active lever press, inactive lever press, or CS probe). Peri-event activity maps (100 ms bin width) were constructed for a 10 s window surrounding each event (from 5 s before to 5 s after active or inactive lever presses; from 2.5 s before to 2.5 s after CS probe presentations). The mean activity was then calculated for each time bin and plotted against event time (see Figure 4A).

We tested for statistically significant time-locked activity with a two-tailed test comparing the maximum or minimum mean activity of a neuron against the null distribution of maximum or minimum mean activity expected by chance. The null distribution was calculated by repeatedly (1000 times) circularly shifting timestamps of activity traces relative to behavioral events by random values. A neuron was considered significantly time-locked if its maximum mean activity was greater than the 97.5th percentile or its minimum mean activity was less than the 2.5th percentile of the null distribution.

The percentage of significant time-locked neurons that were inhibited versus excited were compared with an exact binomial test to determine significance (Figure 4B). The percentage of neurons with significant time-locked activity was compared across the D1 and D15 groups using a Fisher exact test to determine significance (Figure 4D). For all behavioral events (active lever press, inactive lever press, CS probe; Figure S3A), the percentage of neurons with significant time-locked activity was compared across the D1 and D15 groups using a Fisher exact test to determine significance. For the data in Figure 4E, a chi square test comparing the percentage of neurons INH before, INH after, EXT before, EXT after, and NS in the D1 and D15 groups was used to determine significance. This test was followed by post hoc Fisher exact tests (with Bonferroni correction) to separately compare the percentage of neurons in each condition between the D1 and D15 groups.

Activity traces of significantly time-locked neurons (data in Figures 4F and 4D; Figure S3B) were generated by calculating the mean activity across all trials relative to the event of interest (active lever press, inactive lever press, or CS probe). Traces were normalized to the peak activity in the 10 s window.

To compare activity across the D1 and D15 group neurons (data in Figures 4G–4I; Figures S3D, S3E, and S4E), individual neurons were either peak normalized or z-scored (mean and standard deviation calculated across data from entire 1 hour drug-seeking test). A 2-factor mixed ANOVA with group (D1 or D15) as between-subjects factor and time (1 s bins) as within-subjects factor was used to determine significant differences between the groups. Significant interaction effects were followed by post hoc simple main effects tests with Bonferroni correction where appropriate.

To generate a null distribution for comparison to mean activity traces (Figures 4C, 4H, and 4I; Figures S3D, S3E, S4C, and S4E), randomly shifted data was generated by repeatedly (1000 times) circularly shifting timestamps of neural data relative to behavioral events by random values and averaging activity across neurons. We tested for statistically significant differences in activity with a two-tailed test comparing the mean activity of the real data against the null distribution generated at each time bin by randomly shifting the timestamps relative to the recordings. A time bin was considered significant if its activity was greater than the 97.5th percentile or less than the 2.5th percentile of the null distribution (tests corrected for multiple comparisons with Bonferroni correction).

To determine if neural activity following an active lever press was predictive of response latency on the next trial (Figures 5B and 5C), we calculated the trial-by-trial correlation between the peak activity after an active lever press (100 ms bin with highest z-score value in the 5 s window following active lever press) and response latency on the next trial for all neurons. For this analysis, only active

lever presses that were followed by an active or inactive press on the next trial were included (as omission trials have no response latency). Wilcoxon signed rank tests comparing the median of the distribution of correlation coefficients to zero was used to determine significance. A K-S test comparing the correlation coefficients between the D1 and D15 groups was used to determine significance. As a control to determine if activity after the active lever press could be better explained by longer-term changes in calcium activity occurring over the drug-seeking test, we also calculated the trial-by-trial correlation between the peak activity after an active lever press and time in the session (Figures S4G and S4H).

Finally, to confirm that the differences we observed across the D1 and D15 groups were not better explained by differences between individual animals rather than between groups, we also analyzed data with a linear mixed-effects model (function *fitlme* in MATLAB) using group (D1 versus D15) as a fixed-effect and accounting for the multiple neurons from each rat as random effects. For the data in Figure 2L, the model was fit for mean inter-event interval. For the data in Figure 4I, the model was fit for z-scored activity separately at each 1 s time bin. For the data in Figure 5C, the model was fit for the calculated correlation coefficients.

Comparison of activity across behavioral events

To compare activity across multiple behavioral events (Figure S3C), we first balanced the number of trials for each event by selecting a random subset. The number of trials selected was determined by whichever event (active lever press, inactive lever press, CS probe) had the fewest trials. For the data in Figure S3C, a chi square test comparing the percentage of neurons with peak activity across each behavioral event (before active press, after active press, before inactive press, after inactive press, or CS probe) in the D1 versus D15 groups was used to determine significance. This test was followed by post hoc Fisher exact tests (with Bonferroni correction) to separately compare the percentage of neurons in each condition between the D1 and D15 groups.

To compare activity across the two different operant responses (active versus inactive lever press; Figure S3F), a 2-factor repeated-measures ANOVA with lever (active or inactive) and time (1 s bins) as factors was used to determine significance. As rats typically performed few inactive presses, we performed another analysis to account for the difference in number of active versus inactive trials (Figure S3H). Trials were balanced by selecting a random subset of active trials equal to the number of inactive trials. We then calculated the mean activity across trials (1 s bins, 10 s window around time of inactive/active press, peak normalized to highest activity across both events), and inactive press activity was subtracted from active press activity (with 0 - representing no difference in activity, positive numbers representing higher activity relative to active press, and negative numbers representing higher activity relative to inactive press trials). The difference in activity (active - inactive) was averaged across all recorded neurons. This process was repeated (100 times), selecting a different random subset of active press trials on each iteration, to create a distribution of the active - inactive difference. The difference was considered significant if this distribution (2.5^{th}-97.5^{th} percentile) did not contain zero.

We also compared peak activity across the D1 and D15 groups at various behavioral time points in the drug-seeking test (Figures S3G, S4D, and S4F). Peak activity was first determined for each trial, defined as the highest z-score value (100 ms bin) in a designated analysis window (e.g., 5 s before lever press). Peak activity was averaged across all trials for a neuron, and comparisons were made across neurons. For the data in Figure S4D, peak activity was compared between omission and active lever press trials with a paired two-tailed t test. For the data in Figures S3G and S4F, peak activity was compared with a 2-factor mixed ANOVA with group (D1 or D15) as between-subjects factor and event (active/inactive press or active press/omit) as within-subjects factor. Significant interaction effects were followed by post hoc simple main effects tests with Bonferroni correction where appropriate.

Optogenetic activation

For the optogenetic terminal activation experiment, active lever presses, inactive lever presses, omissions, and response latency were compared on stim versus no stim trials for the D1 and D15 groups. For the data in Figure 6E, a 2-factor mixed ANOVA with group (D1 or D15) as between-subjects factor and stimulation condition (stim or no stim) as within-subjects factor was used to determine significance. The same test was used for the control data comparisons in Figure S5B).

As we found no significant interaction between group (D1 and D15) and stimulation condition, we then combined the D1 and D15 groups to compare all ChR2 animals to all YFP control animals (Figure S5E). A 2-factor mixed ANOVA with group (YFP or ChR2) as between-subjects factor and stimulation condition (stim or no stim) as within-subjects factor was used to determine significance. Significant interaction effects were followed by post hoc simple main effects tests with Bonferroni correction to compare the effect of stimulation in the YFP or ChR2 groups individually.

The time courses of active and inactive lever presses were compared on stim versus no stim trials. For the data in Figures 6F, S5C, and S5F, a 2-factor repeated-measures ANOVA with stimulation condition (stim versus no stim) and session time (20 min bins) as factors was used to determine significance.

For the data in Figure S6A, paired two-tailed t tests comparing the number of active and inactive nosepokes during the ICSS session were used to determine significance. For the ChR2 versus YFP comparison, a 2-factor mixed ANOVA with group (ChR2 or YFP) as between-subjects factor and nosepoke (active or inactive) as within-subjects factor was used to determine significance. Significant interaction effects were followed by post hoc simple main effects tests with Bonferroni correction to compare the number of active versus inactive nosepokes in the YFP or ChR2 groups.

For the data in Figure S6B, velocity and percent change in velocity were compared with a 2-factor mixed ANOVA with group (ChR2 or YFP) as between-subjects factor and stimulation condition (stim versus no stim) as within-subjects factor.

DATA AND SOFTWARE AVAILABILITY

MATLAB code for estimating spatial fields using GP regression is available at https://github.com/wittenlab/Spatial-field-estimates-Murugan-et-al-Cell-2017#gp-regression-for-place-field-estimation. The data that support the findings of this study are available from the Lead Contact, I.B.W., upon reasonable request.

Neuron, Volume *103*

Supplemental Information

Increased Cocaine Motivation Is Associated with Degraded Spatial and Temporal Representations in IL-NAc Neurons

Courtney M. Cameron, Malavika Murugan, Jung Yoon Choi, Esteban A. Engel, and Ilana B. Witten

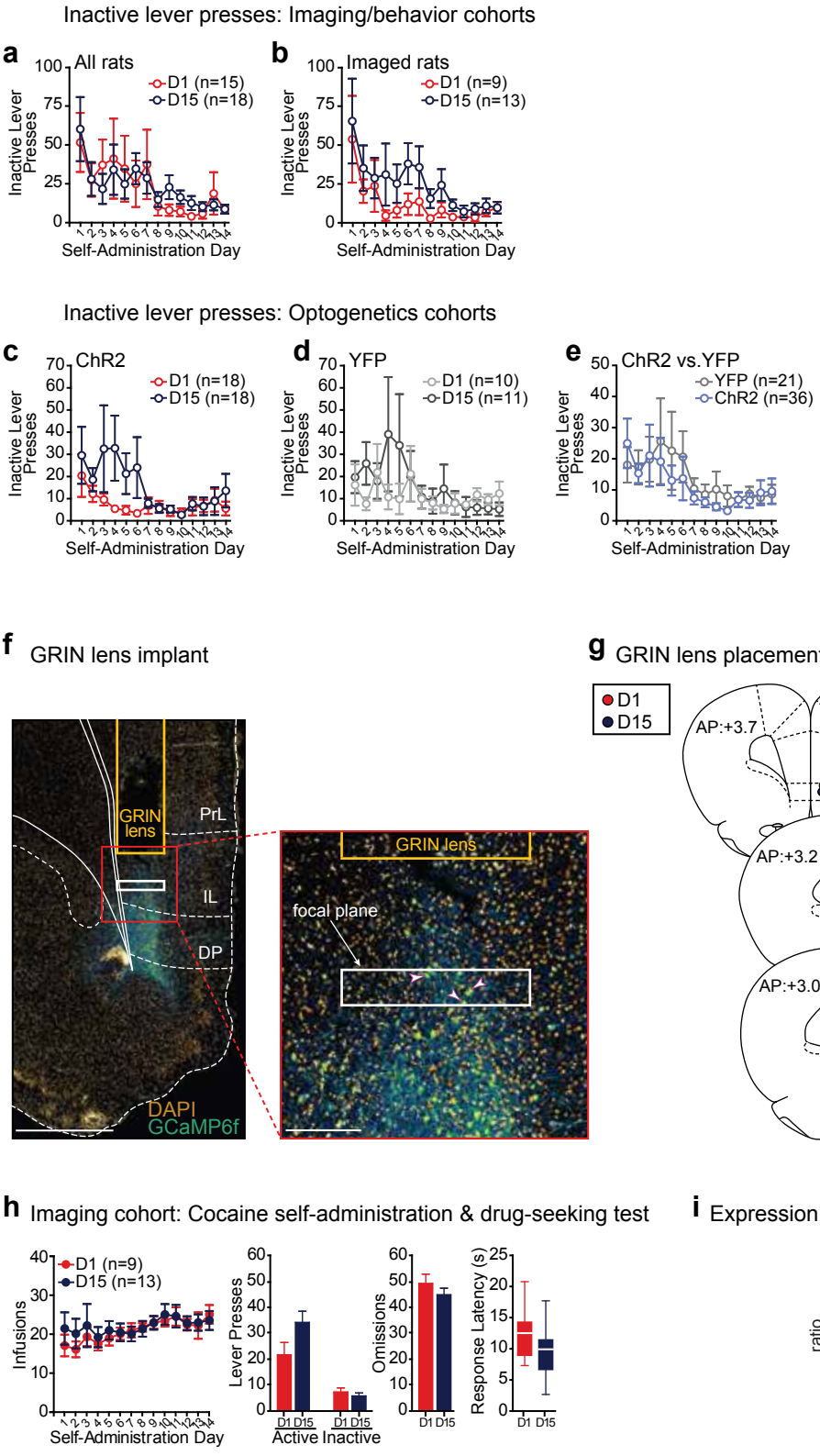

Figure S1. Inactive lever responding and calcium imaging of IL-NAc neurons in rats during drug-seeking behavior, Related to Figures 1 and 2. (a) Over 14 days of cocaine self-administration, rats in the D1 (n=15) and D15 (n=18) groups performed a similar number of inactive lever presses (mean ± sem; main effect of D1/D15 group: $F_{(1,403)}$=0.01, p=0.92), and responding on the inactive lever decreased over the course of training (main effect of time: $F_{(13,403)}$=3.47, p<0.0001). Corresponding active lever presses shown in Fig. 1c. (b) Inactive lever responding (mean ± sem) for the subset of rats from (a) that underwent calcium imaging (D1: n=9, D15: n=13; main effect of D1/D15 group: $F_{(1,260)}$=2.01, p=0.17 ; main effect of time: $F_{(13,260)}$=3.31, p=0.0001). Corresponding active lever presses shown in (h). (c) Inactive lever responding (mean ± sem) for rats in the ChR2 optogenetics cohort (D1: n=18, D15: n=18; main effect of D1/D15 group: $F_{(1,442)}$=2.93, p=0.10 ; main effect of time:

$F_{(13,442)}$=2.08, p=0.014). Corresponding active lever presses shown in Fig. 6d. (d) Inactive lever responding (mean ± sem) for the YFP optogenetics cohort (D1: n=10, D15: n=11; main effect of D1/D15 group: $F_{(1,247)}$=0.38, p=0.55 ; main effect of time: $F_{(13,247)}$=1.18, p=0.30). Corresponding active lever presses shown in Supplemental Fig. 5a. (e) Comparison of inactive pressing (mean ± sem) for all (D1 and D15) ChR2 (n=21) and YFP (n=36) rats (main effect of ChR2/YFP group: $F_{(1,715)}$=0.30, p=0.58; main effect of time: $F_{(13,715)}$=2.76, p=0.0008). Corresponding active lever presses shown in Supplemental Fig. 5a. (f) Left: Histology of GRIN lens placement in the IL, GCaMP6f expression in IL-NAc neurons (green), and DAPI staining of cell nuclei (gold). Prelimbic cortex, PrL; Infralimbic cortex, IL; dorsal peduncular cortex, DP; Scale bar, 1mm. Right: Confocal image showing GCaMP-expressing IL-NAc neurons (denoted by magenta arrows) in the imaging focal plane. Scale bar, 200µm. (g) Histological reconstruction of GRIN lens placements in the IL (red dots: D1, n=9; blue dots: D15, n=13). (h) Cocaine self-administration (main effect of D1/D15 group: $F_{(1,260)}$=0.18, p=0.67) and drug-seeking behavior (active lever press: two-tailed t-test: $t_{(20)}$=1.92; p=0.07; response latency: two-tailed t-test: $t_{(20)}$=1.83; p=0.08) of imaged rats (D1: n=9, D15: n=13). Infusion and lever press data represent mean ± sem. Response latency data represent median (line), 25^{th} and 75^{th} percentiles (box), and minimum and maximum values (bars). (i) The expression of rat-codon-optimized GCaMP6f is 2.70-fold higher than that of standard GCaMP6f as measured by western blot in rat fibroblast cells (mean ± sem, n=3).

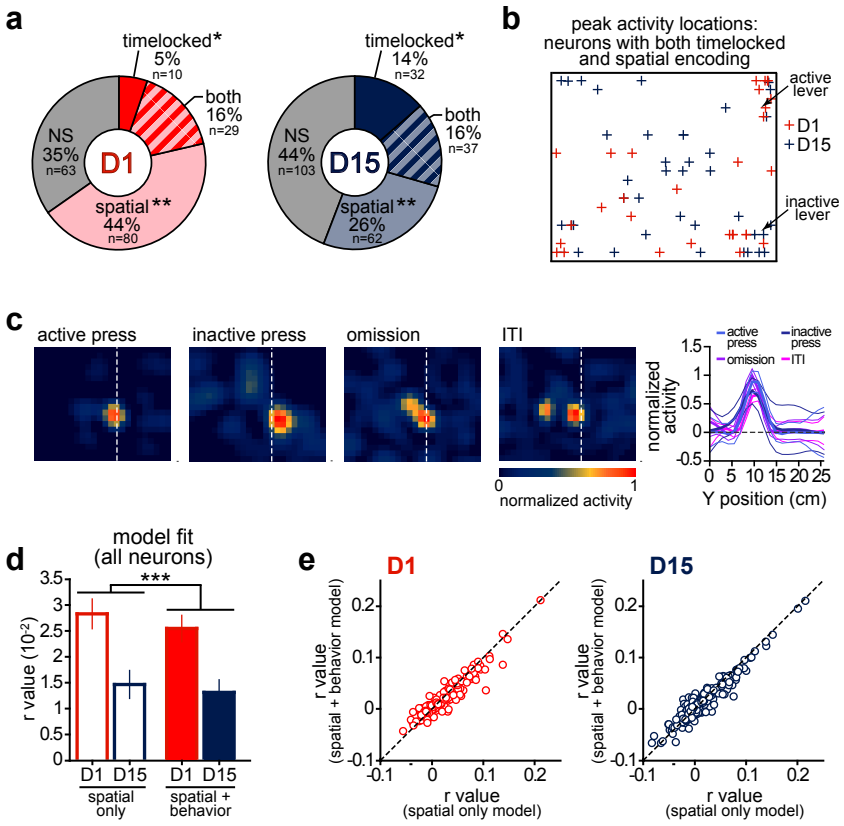

Figure S2. Relationship between timelocked and spatial encoding in IL-NAc neurons, Related to Figure 3. (a) For all neurons (D1: n=182, D15: n=234), the percentage showing timelocked activity, spatial activity, both timelocked and spatial activity, or no significant timelocked or spatial activity (NS) were compared across the D1 and D15 groups. After a longer drug-free period (D15), the percentage of neurons with only timelocked activity was increased, while the percentage of neurons with only spatial activity was decreased (chi-square D1 vs D15: $X^2_{(3)}$=18.20 (n=416), p=0.0004; Fisher exact test D1 vs D15 for timelocked: p=0.032; Fisher exact test D1 vs D15 for spatial: p=0.0012). *p<0.05, **p<0.01. (b) Peak activity locations of neurons with both timelocked and spatial encoding (D1: n=29; D15: n=37). (c) Example spatial fields of a single neuron for different behavior epochs (active press, inactive press, omission, ITI). Line plot (right) represents vertical slice through peak with error bars (± 2STD). Spatial fields were largely consistent across the different behavior epochs. (d) Comparison of model fits (r values) for all recorded neurons (main effect of model type [spatial only versus spatial + behavior]: $F_{(1, 414)}$=11.21, p=0.0009; main effect of D1/D15 group: $F_{(1,414)}$=12.19, p=0.0005. ***p<0.001. (e) Scatterplot of all neurons (D1 left, D15 right) comparing r values for spatial only model versus spatial + behavior model.

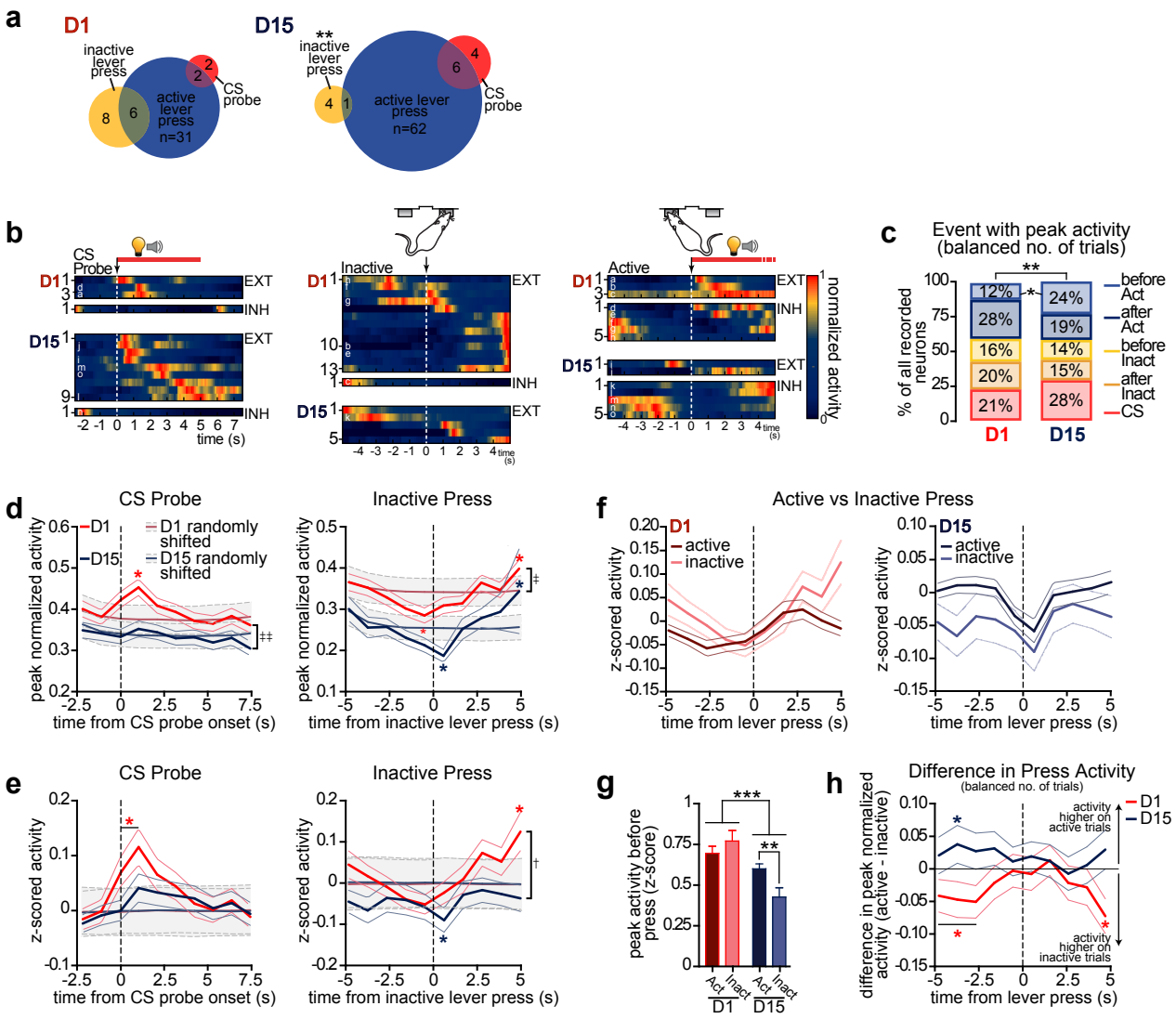

Figure S3. IL-NAc activity is modulated by multiple behavioral events, Related to Figure 4. (a) Venn diagrams showing the number of neurons with significant time-locked activity relative to behavioral events (active lever press, inactive lever press, CS probe) in the D1 (left) and D15 (right) groups. Some neurons had time-locked responses to multiple events. After a longer drug-free period (D15), a smaller percentage of neurons were time-locked to inactive lever press (Fisher exact test D1 vs D15 for inactive lever press: p=0.0087). **p<0.01 (b) Activity traces (normalized to peak) of all neurons with significant time-locked responses relative to CS probe presentation (left; D1: n=3 EXT, n=1 INH; D15: n=9 EXT, n=1 INH) or inactive lever press (middle; D1: n=13 EXT, n=1 INH; D15: n=5 EXT). For neurons which responded to multiple events, corresponding active lever press responses are plotted (right; D1: n=3 EXT, n=5 INH; D15: n=2 EXT, n=5 INH). Letters denote the same neuron across events. Dotted lines indicate CS probe onset (5 s duration) or time of inactive/active lever press. (c) For all neurons (D1: n=182, D15: n=234), mean activity was compared across multiple behavioral events (5 s before active press, 5 s after active press, 5 s before inactive press, 5 s after inactive press, 5 s CS probe presentation) to determine when neurons were most active. 4 neurons in each group had no activity in any of the analyzed event windows and were excluded from this analysis. After a longer drug-free period (D15), the percentage of neurons with highest activity before an active press (relative to other events) was increased (chi-square D1 vs D15: $X^2_{(4)}$=14.89 (n=408), p=0.0049; Fisher exact test D1 vs D15 for before active press: p=0.017). **p<0.01, *p<0.05. (d) Mean ± sem activity (peak normalized) of all recorded neurons (D1: n=182, D15: n=234) relative to CS probe (left) and inactive lever press (right). Randomly shifted data represent mean ± 2SD (1000 iterations). In D1 rats, IL-NAc activity was excited by CS probe presentation. Activity was inhibited around inactive lever presses in both the D1 and D15 groups. Across both events, IL-NAc activity was decreased after a longer drug-free period (D15) compared to the shorter drug-free period (D1) (main effect of D1/D15 group: CS probe: $F_{(1,3726)}$=15.56, p<0.0001; inactive press: $F_{(1,3726)}$=7.75, p=0.0056). *p<0.05, real data compared to shifted. ‡‡p<0.0001, ‡p<0.01. (e) Similar responses were observed with z-scored activity (mean ± sem; left: CS probe, right: inactive press; main effect of D1/D15 group for inactive press: $F_{(1,3726)}$=3.92, p=0.048). Randomly shifted data represent mean ± 2SD (1000 iterations). *p<0.05, real data compared to shifted. †p<0.05. (f) A drug-free period altered the pattern of activity on active vs inactive press trials. Comparison of IL-NAc neural activity (mean ± sem z-score) on all active versus all inactive lever press trials (left: D1, n=182 neurons;

right: D15, n=234 neurons). In D1 animals, activity tended to be higher before inactive lever presses; in D15 animals, activity tended to be higher before active lever presses. This pattern could be the result of the increase in active press-associated activity [(c) & Fig. 4d-g] and/or decrease in inactive press-associated activity [(a), (d, right), (e, right)] observed after a longer drug-free period. (g) Comparison of peak activity (mean ± sem z-score) in the 5 s window before an active or inactive press for all recorded neurons (main effect of D1/D15 group: $F_{(1,414)}$=15.47, p<0.0001; interaction between D1/D15 group and press type (active/inactive): $F_{(1,414)}$=7.54, p=0.0063; simple main effect active vs inactive for D15: p=0.0080). **p<0.01, ***p<0.0001. (h) Difference in activity (peak normalized) for active versus inactive presses comparing equal number of trials. Traces represent mean ± 2SD of difference (active-inactive) across iterations (x100). For each iteration, a different random subset of trials was used. In the D1 group, inactive lever presses were preceded by higher activity than active lever presses. After a longer drug-free period (D15), this pattern was reversed. *p<0.05, different from zero.

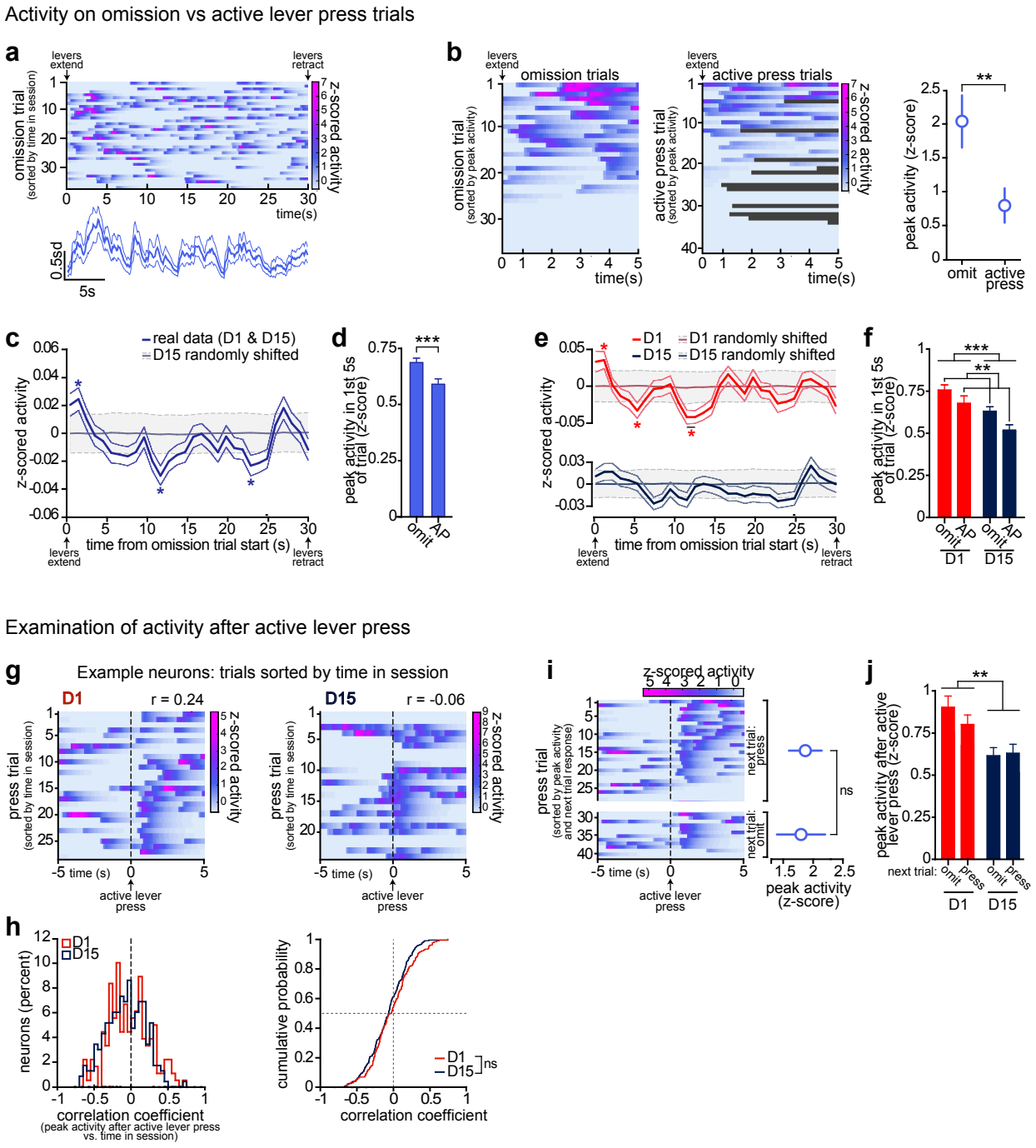

Figure S4. IL-NAc activity is higher at the start of omission trials than at the start of trials on which animals make an active lever press, Related to Figure 5. (a) Example neuron showing activity on omission trials. Heatmap represents z-scored activity in the 30s window from trial start (levers extend) to trial end (levers retract). Trace below shows mean ± sem activity across trials (n=37). (b) Example neuron showing activity at the start of omission trials versus activity at the start of active press trials. Heatmaps represent trial-by-trial z-scored activity during the first 5 s of omission (left) or active press (right) trials (gray indicates trials on which rat responded before 5 s). For this neuron, peak activity across trials (mean ± sem z-score) was higher on omission (n=37) compared to active press trials (n=41) (two-tailed t-test: $t_{(76)}$=2.73, p=0.0078). **p<0.01. (c) Activity was increased at the beginning of omission trials. Mean ± sem z-scored activity of all recorded neurons (n=416) as well as randomly shifted data (mean ± 2SD; 1000 shifted iterations). *p<0.05, real data compared to shifted. (d) Peak activity was higher on average at the beginning of omission trials than at the beginning of active press trials. Comparison of peak activity (mean ± sem z-score) in the first 5 s of omission versus active press trials for all recorded neurons (paired two-tailed t-test: $t_{(415)}$=3.33, p=0.00095). ***p<0.001. (e) Z-scored activity (mean ± sem) of D1 vs D15 neurons (D1: n=182, D15: n=234) during omission trials. Randomly shifted data represent mean ± 2SD

(1000 iterations). Activity was higher at the beginning of omission trials, particularly in D1 animals. *p<0.05, real data compared to shifted. (f) Across the population of IL-NAc neurons, peak activity was higher on average at the beginning of omission trials than at the beginning of active press trials. Comparison of peak activity (mean ± sem z-score) in the first 5 s of omission versus active press trials for all recorded neurons (D1: n=182, D15: n=234; main effect of D1/D15 group: $F_{(1,414)}$=17.70, p<0.0001; main effect of omit vs active press trial: $F_{(1,414)}$=10.45, p=0.0013). ***p<0.0001, **p<0.01. (g) Representative neurons in the D1 (left) and D15 (right) groups show z-scored activity on active lever press trials (dotted line at time of active press). Trials are sorted by time in the drug-seeking test session. Correlation coefficients (r) on top right indicate trial-by-trial correlation between peak z-scored activity after active lever press (5s analysis window) and time in session. (h) Histogram and cumulative density function of correlation coefficients for D1 and D15 neurons. In D15 neurons, there was a negative correlation between peak activity after active lever press and time in the session (median different from zero: Wilcoxon signed rank test: z=-4.10, p<0.0001); however, this relationship was not present in the D1 group (median not different from zero: Wilcoxon signed rank test: z=-1.47, p=0.14), nor were the D1 and D15 groups different from one another (two-sample Kolmogorov-Smirnov K-S test: k=0.09, p=0.33). These data suggest that neural activity tends to decrease over the course of the drug-seeking test session, but these time-dependent changes cannot explain the observed relationship between activity and response latency in the D1 group (see Fig. 5b,c) (i) Activity after active lever press was not predictive of whether animals made an omission or press on the subsequent trial. Left: Representative neuron shows z-scored activity on active lever press trials (dotted line at time of active press). Trials are sorted by next trial response type (press on top, omission on bottom). Right: For this neuron, peak activity across trials (mean ± sem z-score; 5 s window after active lever press) did not differ based on whether the next trial was a press or an omission (two-tailed t-test: $t_{(39)}$=0.15, p=0.88). (j) For all recorded neurons (D1: n=182, D15: n=234), comparison of peak activity (mean ± sem z-score) after an active lever press based on whether the next trial was an omission or a press (main effect of trial type (press/omit): $F_{(1,414)}$=1.32, p=0.25; main effect of D1/D15 group: $F_{(1,414)}$=10.32, p=0.0014). **p<0.01

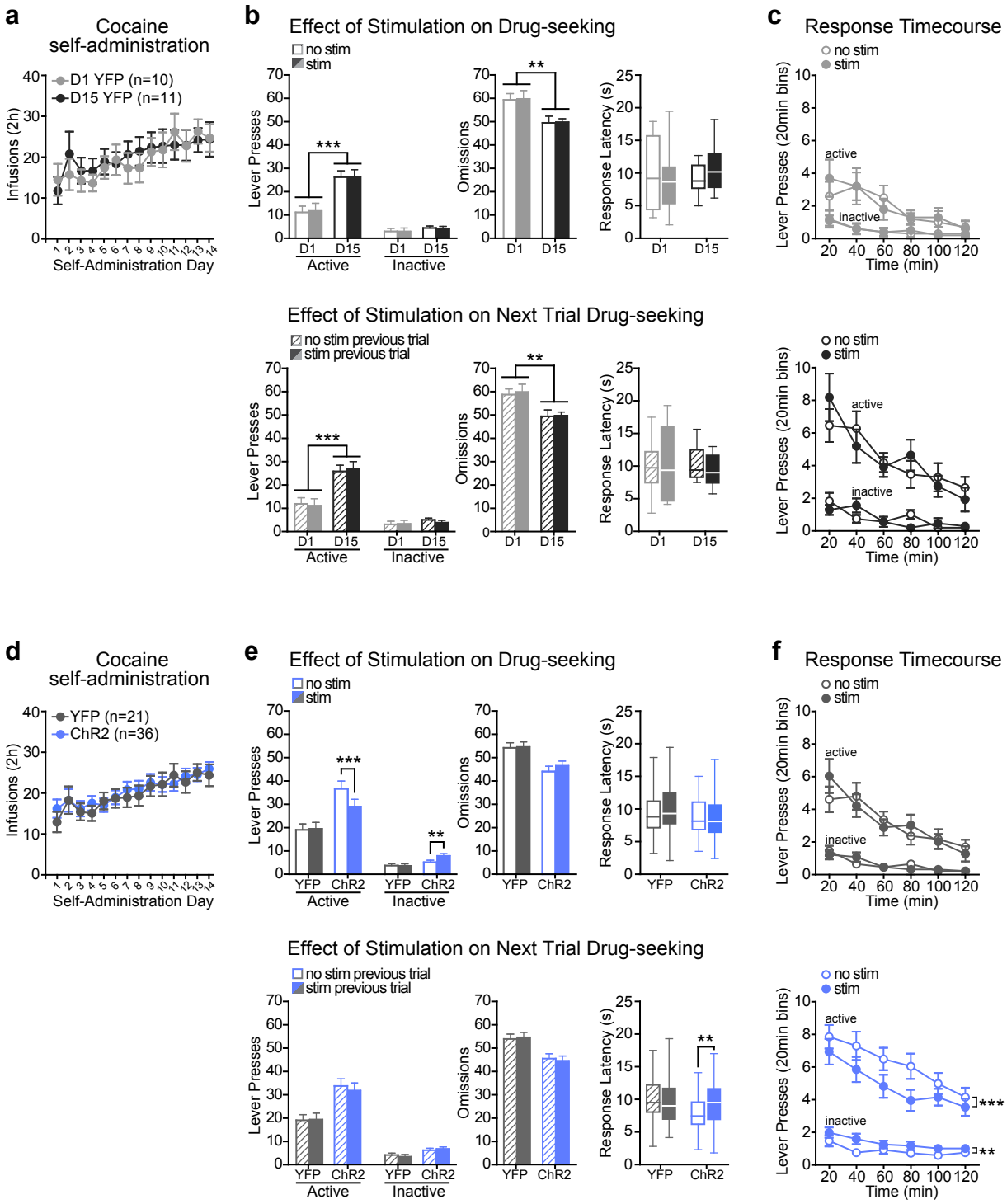

Figure S5. Activation of IL-NAc neurons had no effect on drug-seeking behavior in control animals, Related to Figure 6. (a) Over 14 days of cocaine self-administration, rats in both YFP control groups (D1: n=10; D15: n=11) self-administered a similar number of cocaine infusions (mean ± sem; main effect of D1/D15 group: $F_{(1,247)}$=0.04, p=0.84). (b) Top: Rats that experienced a longer drug-free period (D15) made more active lever presses and fewer omissions ("incubation of craving"; main effect of D1/D15 group for active press: $F_{(1,19)}$=16.11, p=0.0007; main effect of D1/D15 group for omission: $F_{(1,19)}$=13.06, p=0.0018). As expected, activation of IL-NAc neurons with laser stimulation in YFP control animals did not alter active lever pressing (main effect of stimulation: $F_{(1,19)}$=0.11, p=0.74), inactive lever pressing ($F_{(1,19)}$=0.01, p=0.94), omissions ($F_{(1,19)}$=0.03, p=0.87), or response latency ($F_{(1,19)}$=0.28, p=0.60). Bottom: Laser stimulation on the previous trial did not alter active lever pressing (main effect of stimulation: $F_{(1,19)}$=0.04, p=0.85), inactive lever

pressing ($F_{(1,19)}$=0.90, p=0.35), omissions ($F_{(1,19)}$=0.13, p=0.73), or response latency ($F_{(1,19)}$=0.30, p=0.59). Lever presses and omissions are mean ± sem. Response latencies are median, 25th and 75th percentiles (box), and minimum and maximum values (bars). ***p<0.0001, **p<0.01. (c) While animals' response rates decreased over the course of the drug-seeking test (within-session extinction; main effect of time: D1 YFP active: $F_{(5,45)}$=4.56, p=0.0019; D1 YFP inactive: $F_{(5,45)}$=4.12, p=0.0036; D15 YFP active: $F_{(5,50)}$=7.22, p<0.0001; D15 YFP inactive: $F_{(5,50)}$=6.51, p<0.0001), the relative effect of stimulation on active and inactive pressing did not change over time (stimulation x time interaction: D1 YFP active: $F_{(5,45)}$=0.79, p=0.56; D1 YFP inactive: $F_{(5,45)}$=0.15, p=0.98; D15 YFP active: $F_{(5,50)}$=1.30, p=0.28; D15 YFP inactive: $F_{(5,50)}$=2.74, p=0.029, all stimulation main effects tests p<0.05). (d) There were no differences in cocaine intake (mean ± sem infusions) between rats in the YFP (D1&D15 combined: n=21) versus ChR2 (D1&D15 combined: n=36) groups (main effect of YFP/ChR2 group: $F_{(1,715)}$=0.08, p=0.77). (e) Top: Laser stimulation decreased active lever pressing and increased inactive lever pressing in ChR2 animals, but not YFP controls (ChR2/YFP group x stimulation interaction for active press: $F_{(1,55)}$=9.50, p=0.0032; simple main effect of stimulation for ChR2 animals: p<0.0001; group x stimulation interaction for inactive press: $F_{(1,55)}$=4.47, p=0.039; simple main effect of stimulation for ChR2 animals: p=0.0023). ***p<0.0001, **p<0.01. Bottom: Laser stimulation on the previous trial increased response latencies on the next trial in ChR2 animals, but not YFP controls (ChR2/YFP group x stimulation interaction: $F_{(1,55)}$=5.77, p=0.020; simple main effect of stimulation for ChR2 animals: p=0.0053). **p<0.01. (f) While animals' response rates decreased over the course of the drug-seeking test (within-session extinction; YFP active: $F_{(5,100)}$=11.18, p<0.0001; YFP inactive: $F_{(5,100)}$=10.61, p<0.0001; ChR2 active: $F_{(5,175)}$=11.37, p<0.0001; ChR2 inactive: $F_{(5,175)}$=3.95, p=0.002), the relative effect of stimulation on active and inactive pressing did not change over time (stimulation x time interaction: YFP active: $F_{(5,100)}$=1.76, p=0.13; YFP inactive: $F_{(5,100)}$=1.23, p=0.30; ChR2 active: $F_{(5,175)}$=0.91, p=0.47; ChR2 inactive: $F_{(5,175)}$=0.58, p=0.72). For ChR2, main effect of stimulation: active: $F_{(1,100)}$=17.92, p=0.00016; inactive: $F_{(1,175)}$=8.05, p=0.0075. ***p<0.001, **p<0.01.

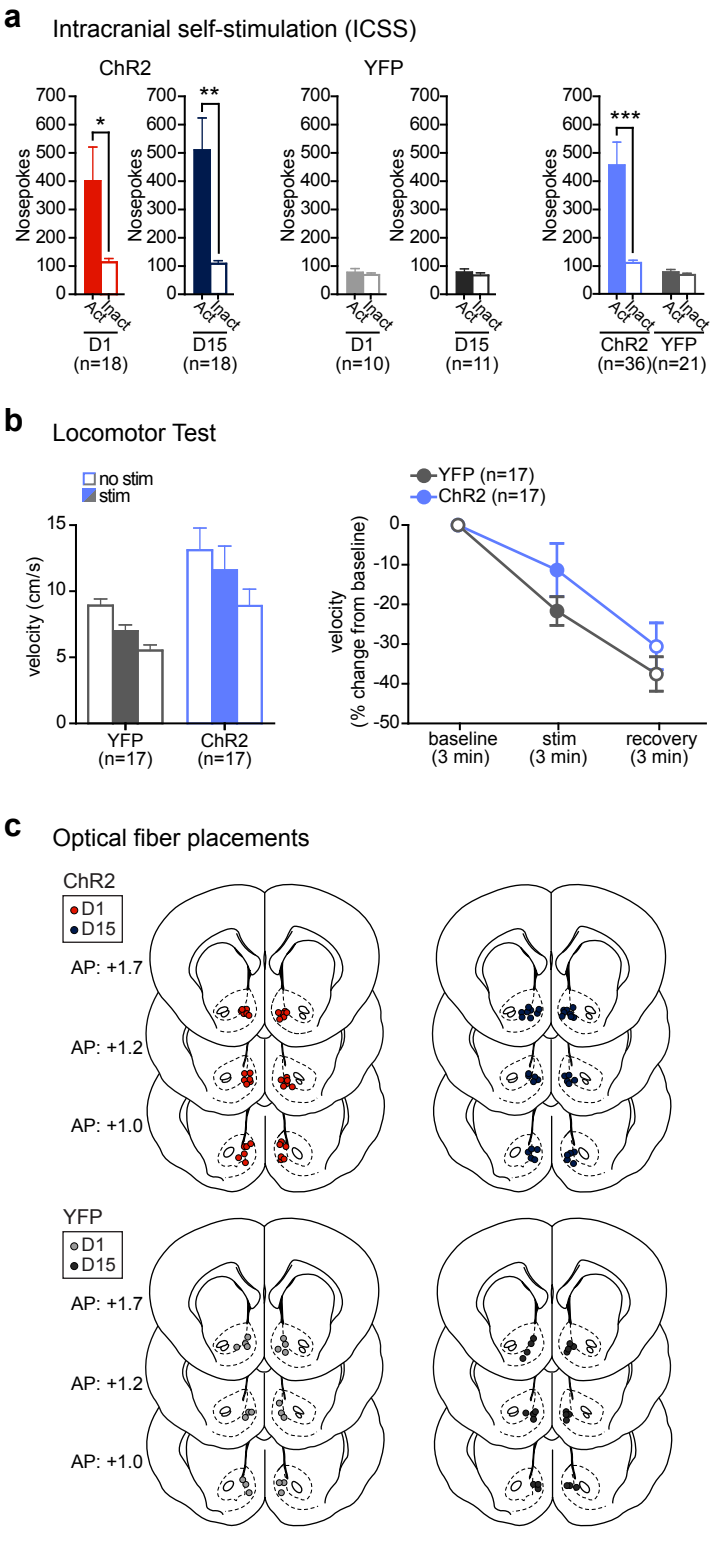

Figure S6. Activation of IL-NAc neurons supports ICSS and does not alter locomotion, Related to Figure 6. (a) Activation of IL-NAc neurons supports intracranial self-stimulation (ICSS). Animals expressing ChR2 made more active than inactive nosepokes during the 4 hour session (paired two-tailed t-test for D1: $t_{(17)}$=2.54, p=0.021; paired two-tailed t-test for D15: $t_{(17)}$=3.65, p=0.0020). YFP control animals had no preference for the active versus inactive nosepoke (D1: t(9)=0.81, p=0.44; D15: $t_{(10)}$=1.12, p=0.29). ChR2/YFP group x nosepoke interaction: $F_{(1,55)}$=10.47, p=0.0021; simple main effect of active vs inactive nosepoke for ChR2 animals: p<0.0001. *p<0.05, **p<0.01, ***p<0.0001. (b) Left: Laser stimulation did not alter velocity compared to control animals in a locomotor chamber. While rats in the ChR2 and YFP groups did have a baseline difference in velocity (main effect of ChR2/YFP group: $F_{(1,64)}$=6.45, p=0.016), laser stimulation affected both groups equally (ChR2/YFP group x stimulation interaction: $F_{(2,64)}$=1.00, p=0.37). Velocity decreased

in both groups over time (main effect of time: $F_{(2,64)}$=36.83, p<0.0001). Right: Similarly, laser stimulation had no effect in ChR2 compared to YFP control animals when considering the % change in velocity from baseline (main effect of ChR2/YFP: $F_{(1,32)}$=1.49, p=0.23; main effect of time: $F_{(1,32)}$=59.71, p<0.0001; ChR2/YFP group x stimulation interaction: $F_{(1,32)}$=0.55, p=0.46). (c) Histological reconstruction of optical fiber tip placements in the NAc shell (red dots: ChR2 D1, n=18; blue dots: ChR2 D15, n=18; light gray dots: YFP D1, n=10; dark gray dots: YFP D15, n=11).